LOW PRESSURE STEAM TURBINE FOR ELECTRICITY GENERATION

BY

SAMUEL ADDO MINTA

(10442803)

THIS THESIS IS SUBMITTED TO THE UNIVERSITY OF GHANA, LEGON IN PARTIAL FULFILLMENT OF THE REQUIREMENTS FOR THE AWARD OF MPHIL PHYSICS DEGREE

JULY, 2015

DECLARATION

This thesis is the result of research work I carried out at the Department of Physics, University of Ghana for my Mphil degree.

References made to other research work and publications are duly cited within the text.

This thesis has not, either in part or in its entirety, been published elsewhere, nor has it been offered for the award of another degree.

Samuel AddoMinta

…… Date……

Supervisors

DR. M.K.A. ADDAE –KAGYAH

…….. Date……

DR. G.K. NKRUMAH-BUANDOH

…….. Date……

DEDICATION

This thesis is dedicated to all my family members for their love, encouragement and care shown to me throughout my education, and also to my wonderful wife Christina Anita AddoMinta and my lovely kids Papa Ekow Nyameaye Addo-Minta and Mame Efua Akyedzi Addo-Minta for their wonderful support and understanding. Indeed I am very much grateful to you.

ACKNOWLEDGEMENT

I would like to express my profound gratitude and thanks to everyone who provided guidance and support throughout this thesis work. In particular, I would like to thank my thesis supervisors, Dr. Michael Addae – Kagyah and Dr. Nkrumah Buandoh for providing the guidance, insight and resources necessary for me to complete this work. I also wish to thank the Head of Department Dr. Amos Kuditcher for his words of encouragement and his contributions made in this thesis work. I am grateful to Mr. Bannerman, Danny, Mr. and Mrs. Abugre and the other teaching assistants for their guidance and support throughout this thesis work, may God richly bless you. Finally, to Mr. Fredrick Tatah and the other technicians in the Department of Physics, I say thank you.

TABLE OF CONTENTS

LIST OF FIGURES

ABSTRACT

In this research work a low pressure steam turbine was designed, constructed and tested for the purpose of studying how electrical power can be generated using low pressure steam from concentrated solar power (CSP) sources. The turbine consist essentially of a two cylindrical casings to which stationary blades are fixed on the inside and a shaft carrying rotating blades (rotors) penetrating between the rows of stators. Steam fed into the turbine passes alternately through the stators and rotors with the stators directing the steam at the right angle for impingement to the rotor blades. A seal was applied to the ends of the casing since the shaft of the rotor passes through the ends of the casings. Leakages were not really eliminated but merely controlled to a minimal level, the shaft of the rotors is attached two bearings, one at each end. The data obtained during the experimental operation of the turbine indicates that temperature is maximum at the beginning, that is at inlet to the first stator blade and is around 88^{o}C and the temperature at the exit of the turbine is 59.5^{0}C. We also observed that steam velocity is maximum at the inlet to rotor blade and the velocity increases as the steam passes through the stator blades. The velocity is also maximum at the exit of the stator blade and decreases as the steam impinges over the moving blade (rotor blade), and thus satisfies condition of Impulse-reaction turbine. The maximum steam velocity at the inlet of the moving blade is 256 m/s and the velocity of steam at the exit of stage is 42 m/s. Again it was also observed that the power output and the thermal efficiency are highest when turbine inlet temperature is increased and the specific steam consumption is least with the increase in turbine inlet temperature. The satisfactory performance at low steam pressure demonstrates that this turbine may be applied in solar-thermal based power generation application where steam pressures are usually low.

CHAPTER ONE

1.0 INTRODUCTION

The major concern of the world at this time is the growing rate of energy consumption as a result of increasing population. Providing adequate energy to developing countries is one of the greatest global technical challenges today. We are living in an era where it is difficult to control the use of energy, for both domestic and commercial purposes. However the more energy we generate using fossil fuel, the more the current pollution crisis is worsened [1]. So the only way left to deal with this situation is to generate electricity with sources of renewable energy, such as solar, wind and tidal waves, as illustrated in figure 1.1 [2].

Fig. 1.1: A photograph of solar panels and wind vanes. (Adapted from Wikipedia, 2012)

1.1 Need of Renewable Energy Production

An individual's ability to produce electrical power in developing rural areas is restricted by the economic limitations of importing energy production machines such as generators and the constant need for fuel input. Solar energy has great promise as an input source because it is widely distributed around the planet and has high energy density. The

current practice for solar energy usage in rural areas is the purchase of photovoltaic systems which are expensive to produce and require specialized silicon fabrication processes. Rural inhabitants need to be able to fabricate solar energy conversion machines locally to reduce dependence on supply sources, and the energy must be produced at a lower cost than what is available [1]. Solar power is a leading contender for the future provision of clean, sustainable and indigenous energy, due largely to the fact that more solar energy falls on the Earth's deserts in 6 hours than the entire population of the planet consumes in a year [2]. Harnessing only a fraction of this available energy would allow the whole world to meet its electricity demand from a clean and sustainable source.

Over the last decades, two dominant solar power technologies have emerged on the international market: solar photovoltaic and solar thermal power [3]. Solar photovoltaic systems convert the Sun's energy directly into electricity, whereas solar thermal power plants use this energy to create a high-temperature heat source, which can then be used to drive conventional power plant equipment. The European Union's Strategic Energy Technology plan [3] contains ambitious targets for the deployment of solar power technology, with a goal of 12% of electricity generated by solar photovoltaics and 3% from solar thermal power by 2020, with provisions for the additional import of solar-generated electricity from North Africa. The International Energy Agency's roadmaps predict an annual world-wide output from solar thermal power plants of between 1000 and 1500 Terawatt Hour of electricity (TWhe) by 2030 [4], with solar photovoltaics contributing another 500 to 1000 TWhe [5], together this corresponds to around 10% of the global electricity supply. The new generation of thin-film photovoltaic panels are

currently the solar power technology that provides the lowest cost of electricity [6]. However, due to the effects of rapidly changing weather conditions and the lack of a large-scale, low-cost technique for electricity storage, their output is both uncontrollable and highly variable. On the other hand, the more expensive solar thermal power plants can take advantage of the thermal conversion step to integrate hybridization and thermal energy storage, and thereby supply reliable and controllable power on demand to consumers. By decoupling the electrical output from the instantaneous solar input, solar thermal power plants can continue to generate electricity during times when the Sun is not shining, such as during inclement weather, or at night [6]. Capable of being deployed on a utility sized multi-megawatt scale, they can benefit from economy of scale effects, which are expected to lead to significant cost reductions through mass production in the coming years.

The growing penetration of variable (i.e. non-controllable) renewable energy sources such as solar photovoltaics and wind into the production mix (currently 13% in Sweden, 18% in Spain and up to 27% in Denmark) is resulting in an increased challenge to maintain the stability of the electricity grid [6]. Rapid transients in power output due to changes in meteorological conditions will need to be compensated for by other, dispatchable, power technologies. The requirement for reserve power generation capacity may place limits on the amount of variable renewables that can be integrated into existing electricity grids. As the share of variable renewable energies in the electricity mix rises, the speedily dispose of solar thermal power plants provides them with a distinctive market opportunity. Almost uniquely amongst renewable energy technologies, they are able to provide a controllable source of power, which will allow

them to play an increasingly valuable role in balancing the fluctuating output of other renewable technologies [7]. In coming years, the solar thermal power industry will need to focus on exploiting the unique opportunities offered by the combination of hybridization and thermal energy storage. As costs fall and the penetration of renewable energies grows, the dispatchability offered by solar thermal power plants will make them ideally suited to forming the cornerstone of a future energy grid based on renewable energy sources.

In Ghana, two large dams situated in the north of Lake Volta produce 1.1 GW of electricity, but the transmission infrastructure reaches only about one quarter of the nation's households so the rest of the country still relies on methods that lead to deforestation – burning everything they can find to generate energy [8]. Therefore In view of this, solar technology will be a viable option that could address the need for rural energy. The successful implementation of small solar steam driven turbines leads to consideration of a mechanical energy economy driven by solar availability. The solar thermal steam powered turbine energy system uses a parabolic collector to concentrate sunlight heat to a boiler. The boiler converts water to steam which exits the boiler at a higher pressure and velocity than the water. The steam acts on a turbine which provides rotational mechanical force. The rotational shaft work can be coupled to those things that require energy – pumps, compressors, grinders, and generators. All components of the system can be made and assembled by ordinary people in a field fabrication laboratory. Because the fabricators have access to the designs and the fabrication tools, they would be able to experimentally optimize the design to meet changing conditions and needs.

1.2 Energy

Proper consideration of energy topics include policy, economics, technology, and analysis. This thesis does not provide policy suggestions or energy plans from a national view but instead considers an alternative, decentralized approach to converting renewable energy to usable energy. Fire provides heat and light. Animals provide mechanical energy. Fire and animals were nearly the entirety of man's energy portfolio until the invention of the steam engine which converts heat energy to mechanical energy. Access to energy leads to a better quality of life. In places where there are no alternatives sources, the motivation for creating energy conversion devices is simply to have adequate energy rather than destroy other fuel sources [11].

1.3 Energy Scheme for Rural Villages

The fastest growing market of solar energy technologies are the third world countries like Ghana with abundant sunlight and a population currently without electricity. Ghana receives 46kWh/m^2 per day and a cumulative 1,800 to 3,000 hours of sunlight per year. Solar radiation is highest in the north of the country which is also the most rural (many villages here do not have a single phone). Developing nations without existing proper infrastructure can benefit from renewable energy technology. As new homes are built in rural areas, they can take advantage of advancements in low energy consumption products and architectural designs for passive management of space heating and cooling. In the conventional view, third world countries view energy as food and heat – something gathered and consumed, while developed nations view energy as a commodity – something measured, stored, purchased and traded [9]. The industrialized energy economy is built around the movement of electrical energy because electrical energy is

easily transported and measured, and can be easily converted to mechanical work or heat [9]. The centralized energy creation scheme appears to work because the conversion from heat to electrical energy can be efficient at larger scales where output heat can be reused. However, cumulative efficiency of the system must take into account the entire electrical power infrastructure including unused electrical losses, source fuel transportation, and waste disposal.

A decentralized approach to providing on demand energy for rural homes requires a scheme for energy storage. This is especially true if the input source is solar, wind, tidal, or any non constant force. Storage capacity must be at least equal to the consumption expected when the sun is below the horizon or winds shift because of local weather. Commonly, rechargeable batteries are used to store electrical energy generated when the sun or wind is present then discharged as the user requires. Batteries are convenient – they are dense and mostly quiet, but do not hold charge indefinitely. Nickelmetalhydride (NiMH) batteries, the most environmentally (and people) friendly rechargeable battery type used in household photovoltaic systems, discharge a few percent per day at 21.1°C. In hot climates (30°C – 40°C), a NiMH battery will self-discharge in one to three months, and in very hot climates (40°C – 50°C) or if the batteries are stored in a space which traps heat, a NiMH battery will self-discharge completely in less than a month [10]. The batteries must be cycled (discharged completely and charged completely) every few months or more, and they lose their ability to be charged over time. The biggest drawbacks to most batteries are their cost, toxic chemical makeup and inability to be locally manufactured at the point of use. Hydroelectric generations from dams are an extreme example of obtaining electricity from potential energy. Scaled to individual

households, this takes the form of pumped storage of water to large water tanks on roof tops. The water is not consumed, it can be collected in an underground or ground level tank then pumped back to the rooftop when the energy source resumes. Importantly, when a household or village outgrows its existing capacity, it gains more capacity by making more conversion devices instead of cutting down more forests. The community's ability to fabricate their own energy devices means access to usable energy without trading their air quality, future resources, or being forced to move closer to cities. The startup rate is much more timely, and rural villager do not need to wait for others to bring, or fund, development to them.

1.4 Solar radiative transfer

The source of the energy that sustain life on Earth is the sun. The basic global energy balance of the Earth is between energy coming from the sun and the energy returned to space by Earth's radiative emission. The absorption of solar radiation takes place mostly at the surface of Earth, whereas most of the emission to space originates in its atmosphere. The energy reaching the Earth's surface in the form of direct or scattered radiation determines the temperature of both the surface and the lower atmosphere, which in turn determines the evaporation capacity and climatic features. The radiation reaching the Earth has different values during the year. This fluctuation results from the Earth's movement in an elliptic orbit and from the obliquity (in relation to the elliptic orbit) of the rotation [12].The first law of thermodynamics states that energy is conserved. The first law for a closed system may be stated as, "The heat added to a system is equal to the change in internal energy minus the work extracted." This law may be expressed mathematically as;

$$dQ = dU - dW \tag{1.1}$$

Where dQ, the amount of heat added, dU is the change in internal energy of the system, and dW is the work extracted from the system. Heat can be transported to and from a system by the processes of Radiation, Convection and Conduction. The transmission of energy from the sun to earth is almost radiative. Figure 1.2 shows the modification of solar radiation by atmospheric and surface processes for the whole earth over a period of one year. Of all the sunlight that passes through the atmosphere annually, only 51% is available at the earth's surface to do work. This energy is used to heat the earth's surface and the lower atmosphere, evaporate water, and run photosynthesis in plants. Of the other 49%, 4 is reflected back to space by the earth's surface, 26% is scattered or reflected to space by clouds and atmosphere particles, and 19% is absorbed by atmosphere gases, particles and clouds.

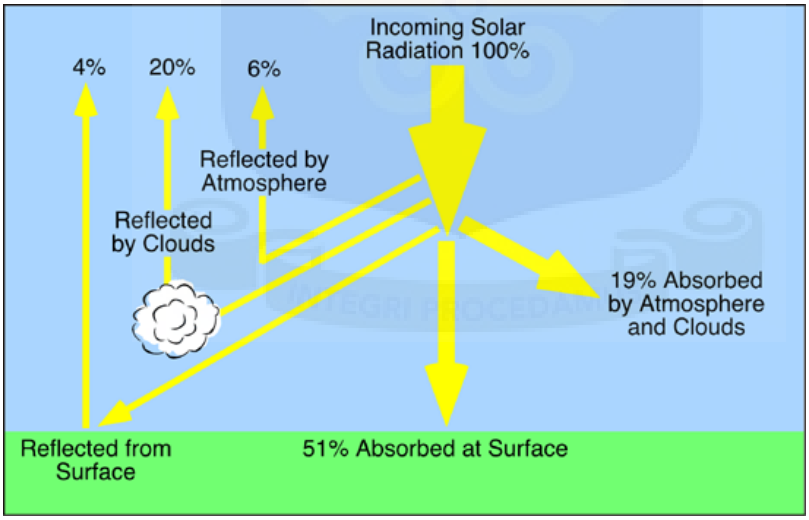

Fig. 1.2 Interactions associated with the absorption and distribution of solar radiation on the Biosphere. (Adapted from Fundamentals of Physical Geography)

1.5 Measurement of solar radiation

The solar radiation that passes through the atmosphere is partially absorbed by the constituents of the atmosphere, partially reflected back to space, and is partially diffused with the remaining reaching the ground as direct solar radiation. Diffuse solar radiation is that solar radiation received from the sun after its direction has been changed by reflection and scattering by the atmosphere. It has no fixed direction at any instant. It is scattered in all directions [13]. Solar radiation consists of electromagnetic radiation emitted by the sun in spectral regions ranging from X-rays to radio waves. The "optical radiation" spectrum with a spectral range of about 300-4000nm in the terrestrial region has applications in renewable energy which utilizes this particular radiation. The determination of this radiation has changed over time with respect to measurements from terrestrial observatories and space borne instruments, modeled calculations or a combination of these[14].The spectral integration of the extraterrestrial solar spectrum over all possible wavelengths (0 to infinity) is usually referred to as the "Solar constant" or "Air mass zero" (AM0) spectrum. Since the sun's output is not constant but varies slightly over short (daily) to long periods, the name total solar irradiance has been introduced [15]. Terrestrial solar radiation measurements are based on pyranometers that respond to radiation with a hemispherical field view, or pyrheliometers, narrow field view of instruments (5.8° to 5.0°) that measure the nearly collimated (i.e. parallel rays) radiation from the 0.5° diameter solar disk and a small part of the sky. The total hemispherical radiation (Global radiation), G, on a horizontal surface is the sum of the direct beam, B, projected on the surface (modified by the cosine of the incidence angle of the beam), I, and the sky radiation (diffuse beam), D. The direct solar radiation is observed from sunrise to sunset, while global solar radiation is observed in the twilight

before sunrise and after sunset, despite its diminished intensity at these times. The expression for these radiations is given as:

$$G = Bcos(I) + D \tag{1.2}$$

Where I is the angle between the solar disk and the normal to the horizontal surface.The direct beam or direct normal solar radiation is measured by a pyrheliometer on a sun-following tracker. The diffuse solar radiation is measured by a shaded pyranometer under a tracking ball, and the global horizontal solar radiation component is measured by a pyranometer with a horizontal sensor.

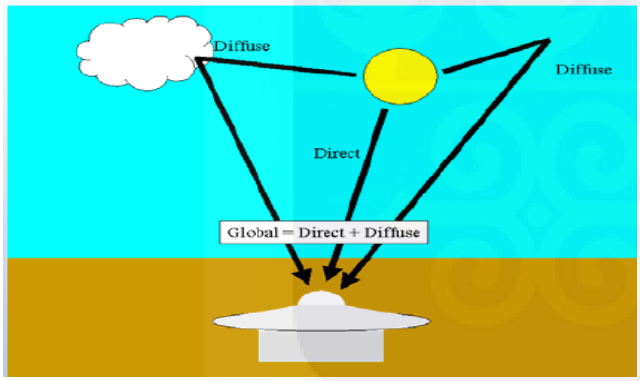

Fig1.3: Distribution of the solar radiation components (Adapted from Stoffel and Wilcox, 2004)

To evaluate system efficiency, it is necessary to measure the input energy. In the system described, heat from the sun is the sole source of input energy. Solar radiation, or the radiant energy emitted from the sun, that hits the earth is a function of the distance between earth and the sun, the condition of the atmosphere, and the latitude of the measurement. Solar irradiance is usually measured with a pyranometer (broad, direct and diffuse contributions of heat) or a pyrheliometer (incident light only) [11]. Pyranometers

respond to the change in temperature when the sunlight heats a black surface, a picture of the pyranometer is indicated in figure 1.4 . The pyranometer gives a voltage signal that is directly proportional to the irradiance as measured in watts per square meter. It is specially designed to accept light from all angles. It has a flat response to light from the ultraviolet to the far infrared, and also has a stable output regardless of sky conditions and changing ambient conditions. These instruments are calibrated once a year since their output can drift [11].

Fig 1.4: Pyranometer for measuring global horizontal radiation. (Adapted from Stoffel and Wilcox, 2004).

The next instrument is the pyrheliometer, figure 1.5. This instrument is used for measuring the direct part of the solar irradiance [16]. Sunlight (the wavelengths of electromagnetic radiation that the sun gives) enters the window and is directed onto a thermopile which converts heat to an electrical signal that can be recorded [17].

Fig. 1.5: showing an Eppley Pyrheliometer, (http://lampes-et-tubes.info/si/si004.php?l=e)

1.6 Solar energy technology

Solar thermal energy delivers more than 3,000 BTU or 100 W to nearly every square foot on the surface of the planet. Solar energy is clean, widely distributed, and densely delivered as compared to other renewable resources. Current solar usage falls into three categories, direct conversion to electricity, thermal collection to generate heat or refrigeration, and thermal collection to generate mechanical work. Direct conversion to electricity is most commonly accomplished with photovoltaic cells. Photovoltaics (PV), which use only a small slice of the solar spectrum, are the most common example of rural home solar energy use but are expensive and inefficient for truly wide spread use [17]. Thermal collection usage for cooking, heating or refrigeration (through evaporative cooling processes) is the crudest form of solar energy and often found in various scales from dinner pot cookers, home heating, and mini refrigerators. Thermal collection and conversion to electricity is mainly experimental and found only in the most industrialized countries where research is focused on large scale deployment in a centralized power generation scheme. Solar motors have been described in history since at least the 1600's.

Modern solar thermal engines typically employ complex engines such as the Stirling engine with hundreds of unique parts requiring true 3D machining and are nearly impossible to make in the field. While these engines are chosen for conversion efficiency, the operating capacity is greatly diminished due to frequent maintenance needs. Intrinsic complexity of the Stirling engines are also reflected in their price tag and build time [15]. Nikola Tesla's boundary layer engine, first patented in 1909, uses fluid to mechanically transfer energy to flat disks which are keyed to a shaft. These flat disks form the working surface of the engine and are significantly easier to produce than conventional curved and flaring turbine blades. The turbine can be scaled to micrometer lengths because adhesion, not impingement, causes momentum transfer between the moving viscous fluids with the disks. [15]

1.7How Boilers Convert Thermal Energy to Kinetic Energy

A steam generator is a heat exchanger used to convert water into steam. The steam is a gas at much higher pressure than the water and the pressure can be converted into mechanical energy. Simply boiling water creates "saturated steam" which can recondense into water quickly. A boiler which further heats the steam creates "superheated steam" at much higher pressures. "Wet steam" is what is commonly seen coming from a boiling kettle and is actually a mix of water vapor and tiny droplets of liquid water. A typical example of a compact steam turbine generator is shown in figure 1.6.

Fig. 1.6: A picture of a Steam generator S201. (Adapted from www.caeasensor.com)

A common steam engine uses the volumetric expansion associated with steam production to move pistons or turbines to perform mechanical work. An intriguing method of steam generation is to drip small amounts of water onto a very hot surface. The resulting "steam explosion" is due to the water flashing into steam very quickly.

1.8 The Basic Principle of a Turbo machinery

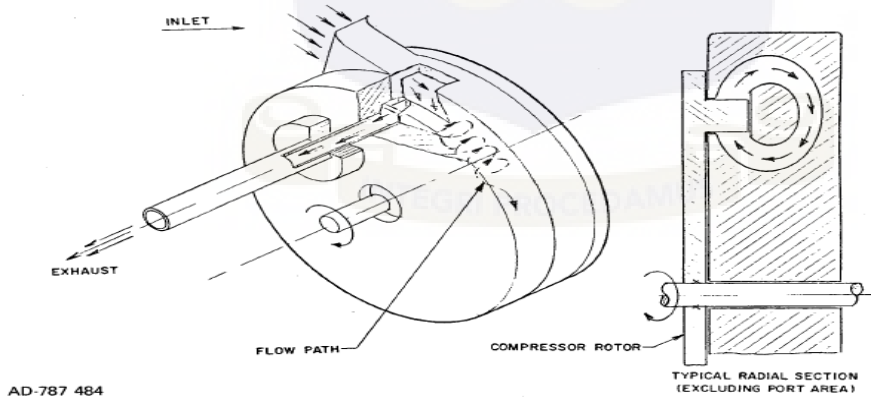

Fig. 1.7: A diagram of a Turbo machine for low temperature application. (Adapted from turbomachineandtools.com)

Turbomachine is a generic term for a device which transfers momentum to and from moving fluids. As illustrated in figure 1.7, a diagram of a turbo machine for low

temperature application, turbines and pumps are both turbo machines. Turbines take energy from moving fluids, usually a gas, and convert it to mechanical rotational "shaftwork" energy. Pumps do the opposite; they transfer mechanical shaftwork energy to the fluid which is usually a liquid. There are three types of turbines, namely reaction, impulse, and drag [12, 13]. Reaction turbines use water pressure pushing on the turbine blades to produce motion, and is an example of Newton's third law of motion. The water pressure changes as it moves through the turbine and gives up its energy. Because water stream will chose the path of least resistance there must be a housing to contain the water in the turbine. Reaction turbines are often used for medium and low head applications with high flow rates. Impulse turbines use the velocity of water hitting the blades causing the blades to move as well as changing the direction of water flow. Impulse turbines are an example of Newton's second law of motion which directly relates the rate of momentum change with the net forces acting on the turbine blade, in the same direction as the external force. Water velocity is the key driver so pressure must be converted to kinetic energy with a nozzle and aimed at the turbine. The impulse turbine is used in very high head applications. Drag or fluid friction turbines use the adhesion of fluid flowing past a rotor surface to drag the rotor into motion. Drag turbines are often used for very low head and high flow rates [12].

1.9 The Boundary Layer Turbine

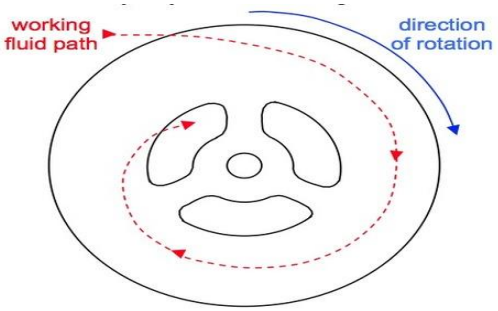

Fig. 1.8: A diagram of a Boundary layer turbine engine. [Adapted from Wikipedia, 2012]

The boundary layer turbine operates differently than a conventional turbine. The boundary layer as illustrated in figure 1.8, the working fluid drags on the rotor, causing momentum transfer by adhesion instead of impingement. Boundary layer turbines are very simple to manufacture, operates without high internal pressures, and tend to fail safely (rather than firing a blade projectile).As fluid moves across a surface, the boundary layer is that first layer of fluid nearest the surface that is slowed by interaction with the surface. The boundary layer force is a viscous force which can be thought of as arising due to fluid friction. The magnitude of the forces interacting between the fluid and the surface are related to the viscosity of the fluid, represented by the fluid Reynolds number. At lower Reynolds numbers, viscous forces dominate and the boundary layer is most effective at momentum transfer. The boundary layer turbine is an old idea. A schematic diagram of a boundary layer turbine is shown in figure 1.8. In 1913 Nikola Tesla patented a turbine based on the friction of fluid flow. It works because of the attachment at the boundary between the immovable, solid blade and the moving fluid. At the very interface between the surface and the fluid, some of the fluid must be slowed down by friction with the surface. The fluid just above the interface would be moving slight faster because it's tangling with something moving slowly. The fluid just about that would be moving slight

faster still. If we plot the velocities of the fluid as a cross section, it is roughly parabolic. This boundary layer is extremely small and usually ignored unless you're dealing with concrete pipes or something very rough, or a very viscous, thick fluid. Tesla's turbines exploit this interaction. The surfaces are shaped as discs about a shaft and as the fluid moves across the surface, it essentially drags the circular blade along with it. Overall turbine efficiency has been estimated at 95% [12] and demonstrated at 41% [13] with a single stage and 70% with multiple stages. The conventional wisdom is that blade less turbines are inefficient compared to the simplest of paddle wheels. This is generally evaluated at the operating point suitable for paddle wheels – high head and variable flows. But bladeless turbines do not make use of all that pressure; the fluid shears and develops only a small adhesion region.

The boundary layer system is more efficient at low flow pressures and momentum transfer efficiency increases as Reynolds number of the fluid decreases. A Tesla engine design as shown in figure 1.9, can have as few as a dozen unique parts and requires only 2D machining, making it ideal for field production. In Tesla's time, the boundary layer engine was difficult to make because thin flat disks could only be made on a lathe where the force of the chuck holding the disk would cause large deformations. Metallurgy at the time was insufficient for high revolutions per minute (RPM), high temperature steam applications. Today, the bladeless boundary layer design is most often used as a pump for viscous, dirty, or difficult fluids. Recently, the bladeless turbine has been employed in applications where the working fluid is contaminated with ash or other residue such as flue exhaust gases [13], with wet "low quality" steam [14], and for pulsatile blood pumping without causing damage to blood parts [15].

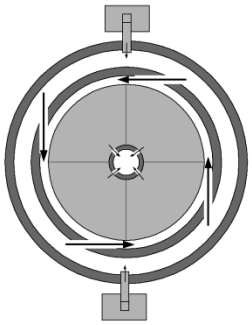

Fig. 1.9: Nikola Tesla's internal combustion engine. [phoenixnavigation.com]

The arrangement of the boundary layer turbine is such that the surfaces are spaced to minimize the regions of laminar flow above the boundary layer. For steam, this spacing is approximately 0.04". For water, the ideal spacing is approximately 0.16". To get the most momentum transfer out of the fluid, we want to expose as much surface area as possible to as much of the fully formed boundary layer as possible. The disks can't be too close together so the boundary layers intersect, and we also don't want to leave too big of a gap or we'll be missing some of the high speed fluid that's rushing past. The exact spacing number depends on the input flow rate and the viscosity of the fluid.

1.10 Motivation for the study

The future belongs to those who can help solve two of our world's most pressing issues, energy and water. -Ron Pernick.

Of the two major world issues, the subject of this dissertation is closely linked to the energy problem with a specific focus on electricity generation using solar power. The energy derived from naturally replenished processes such as wind, tides and geothermal heat is derived directly from the sun, or from heat generated deep within the earth. It is

astonishing when we realize that the earth receives more energy from the sun in just one hour than the world population uses in a whole year [16].Therefore it gives me a lot of joy to embark on such a project to find out how this energy can be effectively used to generate electricity.

1.11 Objectives of this project

- To design and construct a very simple low pressure steam turbine
- Use the turbine in solar-thermal based power generation application where steam pressures are usually low.
- To use the turbine to generate some amount of electrical power.

1.12 Scope of this project:

This project propose the design and construction of a very simple and handy low pressure steam turbine using only local materials which would depend solely on solar radiation for its operation. The turbine is going to be used to generate electricity to power low voltage electrical devices.

1.13 Literature review

A steam turbine is a thermal motor with external combustion, functioning according to the thermodynamic cycle Clausius-Rankine as seen in Figure 1.10

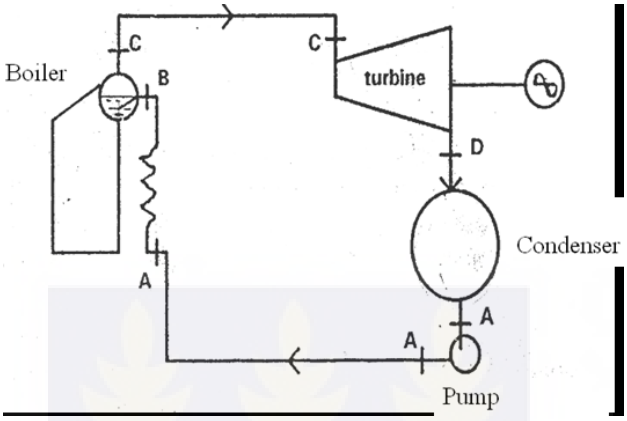

Fig. 1.10 Clausius-Rankine cycle (Adapted from Wikipedia, 2012)

This Clausius-Rankine cycle is distinguished by the state change affecting the motor fluid that is the water steam. Turbine constitutes an evolution exploiting principal's advantages of turbo machines: mass power and elevated volume power; improved efficiency by the multiplication of detente floors [18]. A turbine is constituted of a rotor composed of a tree on which is fixed the dawns and a stator composed of a structural cover of the stationary deflectors, generally organized of two parts according to an axial plan [19]. The turbine is composed besides of a segmented admission tore and a controlled exhaust divergent toward the condenser. The stationary deflector function is to assure all or one of the detente while forming a nozzles network and to modify the direction of the out-flow retiring of the previous floor [20]. A steam turbine is composed of one or several floors assuring each two functions:

1. The steam detente that corresponds to the conversion of the potential energy to kinetic energy; 2. The conversion of the kinetic energy in rotation couple of the machine by the mobile aubages.

The steam turbines are often classified in two big categories combined in the same machine:

1. Turbines to action in which the détente makes himself solely in the stationary aubages. They are well adapted to strong pressure floors and are better suitable to the debit regulation. Their construction is more expensive and their use for the first floors.

2. The jet-propelled turbines in which the detente is distributed between stationary and mobile aubages. The degree of reaction is defined by the distribution of the detente between aubages. They are better suitable for bass pressure floors and their cost is weaker. The realization of turbines requires the recourse to greatly allied steels (Cr-Ni-Va) to resist the thermal, mechanical constraints (centrifugal force) and chemical (steam corrosion). The first two constraints limit the diameter and therefore the capable debit of the last floors. Consequently, a meter of length already creates serious problems of realization. Besides, the radial heterogeneity of speeds imposes a variable impact of the dawn that present then a left shape whose machining is complex [21, 22]. In practice, the temperature is limited to 540°C. The pressure is 180 bars. The turbines used in the electricity production center of Radès (Figure 2) are composed of strong power on a one same axis (disposition tandem compound):

1. High pressure turbine (HP);

2. Intermediate pressure turbine with soutirages (IP);

3. Low pressure turbine with soutirages (LP).

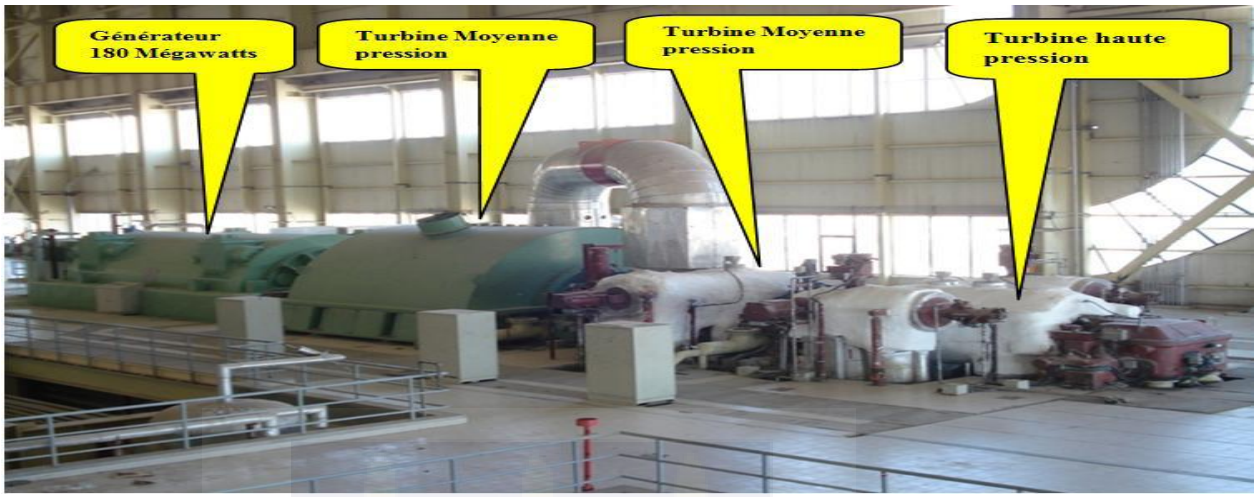

Fig.1.11 Disposition of the turbines at the electricity production center of Radès.(Causal analysis and calculation of the steam turbine efficiency of a thermal power plant - M. N. Lakhoua)

It is thus possible to reach an efficiency passing slightly 40% [23]. The principal favor of steam turbines as shown in figure 1.11 is to be external combustion motors. Of this fact, all fuels (gas, fuel-oil, coal, vestigial, geothermal heat) can be supplied it with steam [24]. The efficiency can reach some elevated values and reduced working expenses (specific consumption of 2300and 3400 kcal/kWh for gas turbines). On the other hand, the cost and the complexity of facilities are the most often reserved to the elevated power facilities. But in particular cases, motors and gas turbines are better adapted below about 10 MW.

1.13.1 Efficiency calculation of steam turbines

The calculation of the efficiency of bodies of the turbine with the difference enthalpy method is very useful for the assessment of the cleaning degree of the steam course in the body of the turbine. The efficiency of the turbine is defined as the report between the real difference enthalpy (DHRHP) and the isotropy difference enthalpy (DHIHP) of steam crossing the HP body. For the BP body this method is not applicable because of the title of steam to the BP exit (humid steam). The efficiency of the HP body (η_{HP}) is defined as follows:

$$\eta_{HP} = \frac{D_{HRHP}}{D_{HIHP}} \quad (1.3)$$

The real enthalpy difference in the HP body is given by:

$$D_{HRHP} = H_{vap} - H_{erh} \text{ (kcal/kg)} \quad (1.4)$$

H_{vap}: enthalpy of steam overheated admission HP turbine.

H_{erh}: enthalpy of steam to overheat HP exit. The difference isotropy enthalpy in the HP body is given by:

$$D_{HIHP} = H_{vap} - H_{ith} \quad (1.5)$$

H_{ith}: final enthalpy of steam overheated for an expansion isotropy (S = constant) of the admission until exit of the HP turbine. In addition, the indicated thermodynamic losses appear in the machine external energy losses provoked mainly by rubbings of mechanical landings furniture and flights. The efficiency of the turbine must take into account these losses.

CHAPTER TWO

2. 0 THEORY

A steam turbine is a device that converts the thermal energy of steam into mechanical energy by using it to turn the blades of a rotor. High-temperature, high-pressure steam passes through a nozzle or fixed blades and spurts out and expands, or has its direction altered into a high-speed jet that is directed against rotor blades which spin the shaft to which they are attached, creating rotational energy.

2.1 Thermodynamics of steam turbine

The steam energy is converted mechanical work by expansion through the turbine. The expansion takes place through a series of fixed blades (nozzles) and moving blades each row of fixed blades and moving blades is called a stage. The moving blades rotate on the central turbine rotor and the fixed blades are concentrically arranged within the circular turbine casing which is substantially designed to withstand the steam pressure. Figure 2.1 illustrates two turbine cylinders tandem mounted.

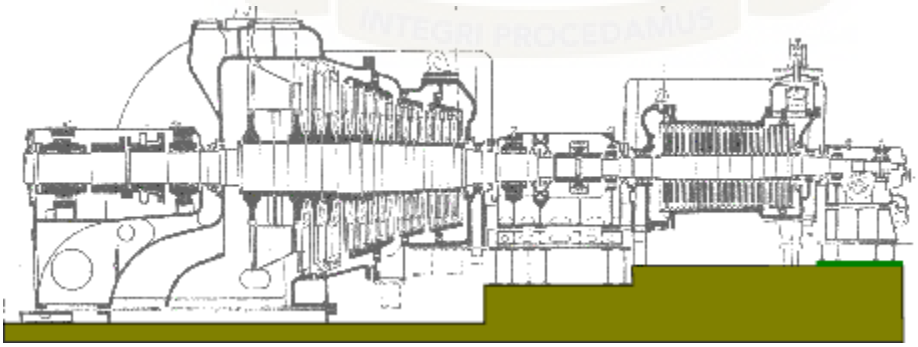

Fig. 2.1: Two Turbine Cylinders Tandem Mounted (Adapted from Wikipedia 2012)

The Rankine cycle is a steam cycle for a steam plant operating under the best theoretical conditions for most efficient operation. This is an ideal imaginary cycle against which all other real steam working cycles can be compared.

The theoretic cycle can be considered with reference to the figure below. There will no losses of energy by radiation, leakage of steam, or frictional losses in the mechanical components. The condenser cooling will condense the steam to water with only sensible heat (saturated water). The feed pump will add no energy to the water. The chimney gases would be at the same pressure as the atmosphere. Within the turbine the work done would be equal to the energy entering the turbine as steam (h_1) minus the energy leaving the turbine as steam after perfect expansion (h_2) this being isentropic (reversible adiabatic) i.e. (h_1- h_2) as indicated in figure 2.2 and figure 2.3. The energy supplied by the steam by heat transfer from the combustion and flue gases in the furnace to the water and steam in the boiler will be the difference in the enthalpy of the steam leaving the boiler and the water entering the boiler = (h_1 - h_3).

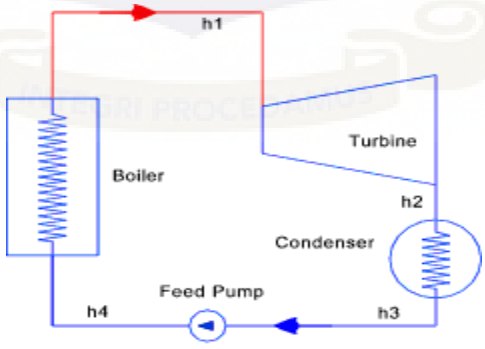

Fig. 2.2: Basic Rankine Cycle (John F. Lee, "Theory and Design of steam and Gas Turbines", 1954)

The ratio output work / Input by heat transfer is the thermal efficiency of the Rankine cycle and is expressed as ;

$$\text{Rankine Thermal Efficiency} = \frac{H_1 - H_2}{H_1 - H_3} \quad (2.1)$$

Although the theoretical best efficiency for any cycle is the Carnot Cycle the Rankine cycle provides a more practical ideal cycle for the comparison of steam power cycles (and similar cycles). The efficiencies of working steam plant are determined by use of the Rankine cycle by use of the relative efficiency or efficiency ratio as below:

$$\text{Relative efficiency} = \frac{Therma\ efficiency\ of\ actual\ plant}{Thermal\ efficiency\ of\ Rankine\ Cycle} \quad (2.2)$$

The various energy streams flowing in a simple steam turbine system as indicated in the diagram below. It is clear that the working fluid is in a closed circuit apart from the free surface of the hot well. Every time the working fluid flows at a uniform rate around the circuit it experiences a series of processes making up a thermodynamic cycle. The complete plant is enclosed in an outer boundary and the working fluid crosses inner boundaries (control surfaces).. The inner boundaries define a flow process. The various identifiers represent the various energy flows per unit mass flowing along the steady-flow streams and crossing the boundaries. This allows energy equations to be developed for the individual units and the whole plant. When the turbine system is operating under steady state conditions the law of conservation of energy dictates that the energy per unit mass of working agent entering any system boundary must be equal to the rate of energy leaving the system boundary [25].

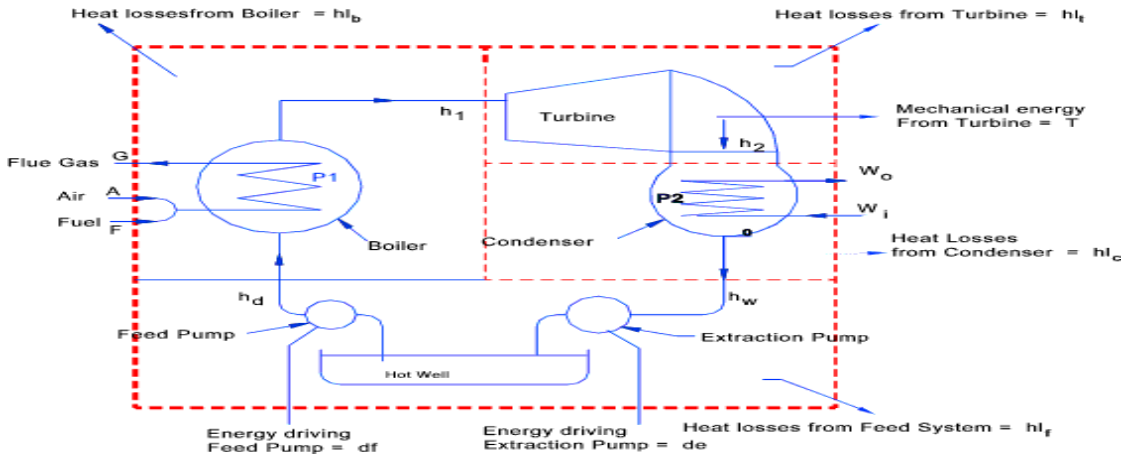

Fig. 2.3: A diagram showing the steady flow energy. (Atrens A, M. Muer, H. Meyer, G. Faber, and M.O. speidel, "BBC Experience with Low – Pressure Steam turbine", Sept. 1981)

2.2 Steady Flow Energy Equations

Boiler

The energy streams entering and leaving the boiler unit are as follows:

$$F + A + h_d = h_1 + G + hl_b \quad (2.3)$$

Hence;

$$F + A = G + h_1 - h_d + hl_b \quad (2.4)$$

Turbine

The energy streams entering and leaving the boiler unit are as follows:

$$h_1 = T + h_2 + hl_t \quad (2.5)$$

Hence;

$$T - h_1 + h_2 + hl_t = 0 \quad (2.6)$$

Condenser Unit

The energy streams entering and leaving the boiler unit are as follows:

$$W_i + h_2 = W_o + h_w + hl_c \quad (2.7)$$

Hence;

$$W_i = W_o + h_w - h_2 + hl_c \quad (2.8)$$

Feed Water System

The energy streams entering and leaving the Feed Water System are as follows:

$$h_w + d_e + d_f = h_d + hl_f \quad (2.8)$$

Hence;

$$d_e + d_f = - h_w + h_d + hl \quad (2.9)$$

The four equations on the right can be arranged to give the energy equation for the whole turbine system enclosed by the outer boundary as;

$$F + A\,Wi + de + d_f = G + T + Wo + \Sigma hl \quad (2.10)$$

Therefore;

$$F = [T- (de + d_f)] + [G – A] + [Wo – Wi] + \Sigma hl \quad (2.11)$$

That is per unit mass the of working agent (water) the energy of the fuel (F) is equal to the sum of;

- the mechanical energy available from the turbine less that used to drive the pumps $T - (d_e + d_f)$

- the energy leaving the exhaust [G - A] using the air temperature as the datum.

- the energy gained by the water circulating through the condenser $[W_o - W_i]$

- the energy gained by the atmosphere surrounding the plant Σh_l

The overall thermal efficiency of a steam turbine plant can be represented by the ratio of the net mechanical energy available to the energy within the fuel supplied. as indicated in the expressions below;

$$\eta_o = \frac{Net\ output\ of\ shaft\ work}{Calorific\ value\ of\ fuel} = 1 - \frac{Energy\ rejected}{Energy\ Supplied} \quad (2.12)$$

$$\eta_o = \frac{T-(de+df)}{F} = 1 - \frac{[(G-A)+(Wo-Wi)+\Sigma hl}{F} \quad (2.13)$$

2.3 Turbine Vapour Cycle on T-h Diagram

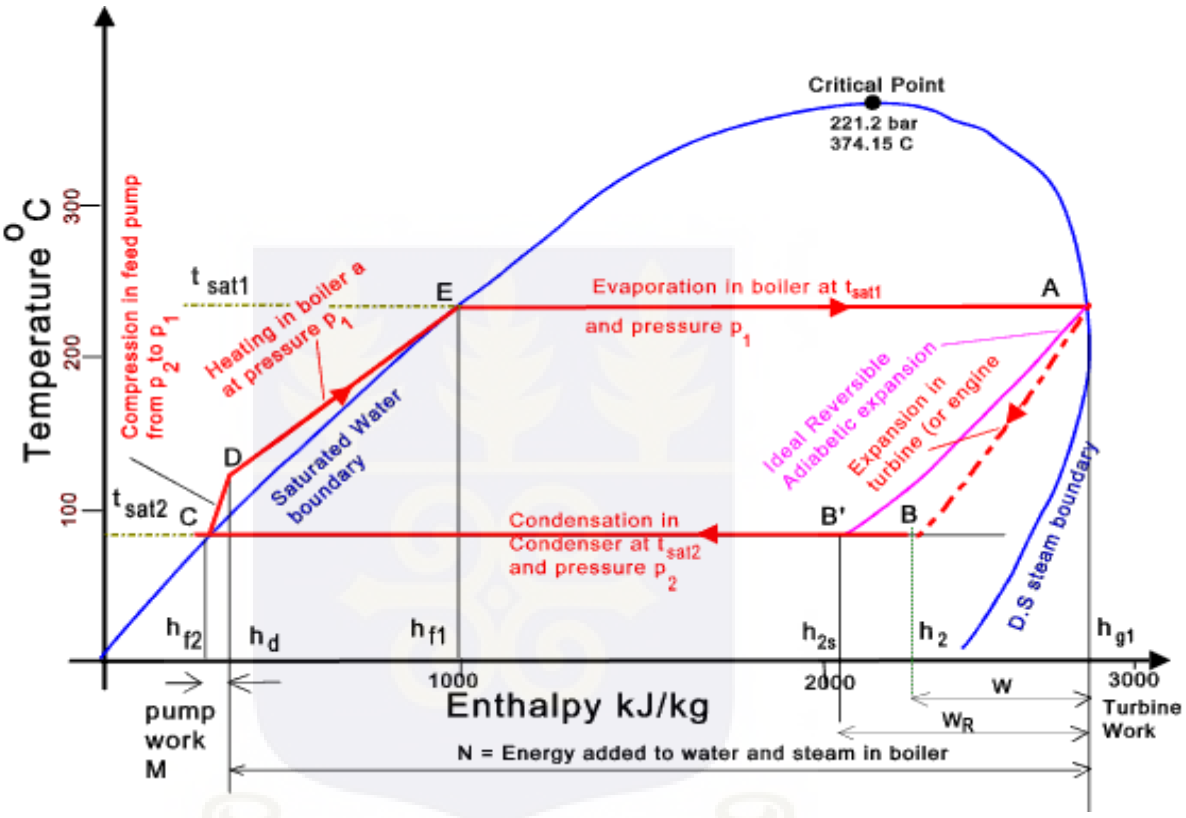

Fig. 2. 4: Steam cycle on Temp - Enthalpy Diagram, (Atrens A, M. Muer, H. Meyer, G. Faber, and M.O. speidel, "BBC Experience with Low – Pressure Steam turbine", Sept. 1981)

The cycle in figure 2.4 shows the stages of operation in a turbine plant. The enthalpy reduction in the turbine is represented by A ->B . The reversible process for an ideal isentropic (reversible adiabatic) is represented by A->B'. This enthalpy loss would be ($h_{g1} - h_2$) in the reversible case this would be ($h_{g1} - h_{2s}$). The heat loss by heat transfer in

the condenser is shown as B->C and results in a loss of enthalpy of (h_2- h_{f2}) or in the idealized reversible process it is shown by B'-> C with a loss of enthalpy of (h_{2s}- h_{f2}). The work done on the water in extracting it from the condenser and feeding it to the boiler during adiabetic compression C-> D is (h_d - h_{f2}) = length M.The energy added to the working agent by heat transfer across the heat transfer surfaces in the boiler is (h_{g1} - h_d) which is approx. (hg1- h_{f2})

The Rankine efficiency of the Rankine Cycle AB'CDEA is

$$\eta_R = \frac{h_{g1-h_{2s}}}{h_{g1-h_{f2}}} = \frac{W_R}{N} \qquad (2.14)$$

The efficiency of the Real Cycle is;

$$\eta = \frac{h_{g1-h_2}}{h_{g1-h_{f2}}} = \frac{W}{N} \qquad (2.15)$$

2.4 Theory and operation of a low pressure turbine and blade design

Steam turbines are the core elements of the steam turbine power plants (Heat power plants). They form the harvesting components of the plant in which the energy of the hot fast and high pressure stream of steam is first transformed into kinetic energy by expansion through nozzles and the kinetic energy of the resulting jet is converted into force doing work on rings of blading mounted on a rotating disc. Steam turbines have four important elements. [18, 19]

1. The nozzle, that is where the steam enters the turbine
2. The stator, in which the energy of steam is converted into kinetic energy, hence into flow of high momentum.

3. The rotor blades, in which the high momentum stream of steam is forced to change direction and so reducing its momentum.

4. The exhaust, where the steam leaves the system.

The difference in momentum is a force applied to the rotor blades forcing them to rotate. These blades are attached to the rotating shaft (wheel), hence transforming this force to torque and then to power acting on the shaft. The rotor blades are the critical elements of the turbine. They carry the entire flow loading. To design such a blade, the designer needs to calculate the flow properties at first estimate the flow forces and evaluate the stresses on the blades.

Blade Loading: the loading on a rotating turbine blade is composed of:

1. Centrifugal forces due to rotation

2. Bending forces due to the fluid pressure and change of momentum

3. Bending forces due to centrifugal action if the centroids of all sections do not lie along one radial line.

The steady stress at any section of a parallel sided blade is a combination of direct tension due to centrifugal forces and bending due to steam force. Both of which are acting on that portion of blade between the section under consideration and the tip. The direct tensile stress is maximum at the blade root and is decreasing towards the tip [20]. The centrifugal stress depends on the mass of material in the blade, blade length, rotational speed and the cross sectional area of the blade. However the impulse turbine blades are subjected to bending stresses as a result of the centrifugal forces, the tangential force exerted by the fluid on the blade and if the centriods of all blades sections do not lie along the same radial line, an additional load is created. The reaction blades have an additional

bending stresses resulting from the large axial thrust as a result of the pressure drop occurring in the blades passage. All turbine blades are subjected to vibration loads and hence, to stress due to vibration. It is worth mentioning that the bending stresses are also maximum at the blade roots. The combined tensile and bending stress is, hence maximum at the root and diminishes with radius. The centrifugal stresses are more significant than other stresses as they have the greatest effect on total stress. Centrifugal stresses are a function of the mass of the material in the blade, blade length, cross-sectional area of blade (profile area) and rotational speeds. To calculate the centrifugal stresses on a moving blade, considering a single blade fixed to the disc as shown below;

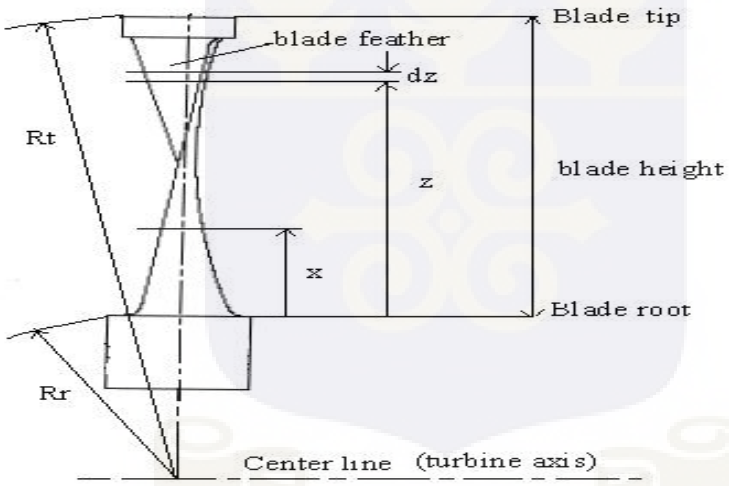

Fig. 2.5: A diagram showing the various parts of a turbine blade, adapted from Atrens A, M. Muer, H. Meyer, G. Faber, and M.O. speidel.

As illustrated in figure 2.5, let Rr be the radius of blade at root section, and Rt be the radius at the tip. The area of the blade profile in section (x) may be denoted as A(x). Let x be an axis of chosen along the blade so as to pass through the axis of rotation of the rotor. It is assumed that the centers of gravity of all blade sections lie on the axis (x). The centrifugal stresses at the blade section are the centrifugal force in this section divided by the area of the blade section, and can be found by formula:

$$\sigma_{ef}(x) = \frac{Fef\ (x)}{A(x)} \tag{2.16}$$

If an infinitesimal element (dz) be separated in section (z) shown in the above figure. The force developed by this element during disc rotation is therefore:

$$dF_{ef} = dm.\omega^2\ (Rr + z) \tag{2.17}$$

$$dm = \rho.\ A\ (z).dz \tag{2.18}$$

Substituting Eq. (2.18) into Eq. (2.17) gives the centrifugal forces in this element [20].

$$dF_{ef}\ (x) = \int_x^{Lb} \rho.\omega^2 A(z).\ (Rr\ +\ z).dz \tag{2.19}$$

By integrating Eq (2.19) the centrifugal force becomes

$$F_{ef}\ (x) = \int_x^{Lb} \rho.\omega^2 A(z).\ (Rr\ +\ z).dz \tag{2.20}$$

Where; Lb = Rt – Rr

The stresses from the centrifugal forces in a blade of arbitrary profile can be determined by the relationship.

$$\sigma_{ef\,(}x) = \frac{\omega^2}{A(x)}[\rho.\int_x^{Lb} A(Z).\ (Rr + Z).dz \tag{2.21}$$

Since the blade has a variable cross-sectional area, to find the centrifugal force, it is necessary to formulate the change of the cross-sectional area as a function of blade height. Using the relation [21].

$$A\ (z) = Ar - (Ar - At)\ (\frac{Z}{Lb})^{\text{Ʀ}} \tag{2.22}$$

Where;

$$\text{Ʀ} = \frac{\ln\frac{(Ar-At)}{Ar-Am}}{\ln 2} \tag{2.23}$$

The centrifugal force on the blade is determined by using Eq. (2.22) and Eq. (2.20) to give;

$$F_{ef}(x) = \rho\omega^2 \int_x^{Lb} [Ar - (Ar - At)(\frac{Z}{Lb})^{Ŗ}](Rr + Z)dz \quad (2.24)$$

And

$$F_{ef}(x) = \rho.\ \omega^2[Ar(Rr.Z + \frac{Z^2}{2})\frac{(Ar-At)}{Lb^{Ŗ}}(\frac{Rr.Z^{Ŗ+1}}{Ŗ+1} + \frac{Z^{Ŗ+2}}{Ŗ+2})]_x^{Lb} \quad (2.25)$$

When x = Lb, at the tip of the blade, the centrifugal force is zero. While at the root section of the blade, where x = 0 the centrifugal force is maximum and Eq. (2.24) becomes:

$$F_{ef}(x) = \rho.\ \omega^2[Ar.Lb\ (Rr + \frac{Lb}{2}) - (Ar - At)(\frac{Rr.Lb}{Ŗ+1} + \frac{Lb^2}{Ŗ+2})] \quad (2.26)$$

The centrifugal stresses are determined by using Eq. (2.25) to determine the force divided by the area given by Eq. (2.20) and the maximum centrifugal stress at blade root becomes;

$$\sigma_{ef}(0) = \rho.\ \omega^2[Lb\ (Rr + \frac{Lb}{2}) - (1 - \frac{At}{Ar})(\frac{Rr.Lb}{Ŗ+1} + \frac{Lb^2}{Ŗ+2})] \quad (2.27)$$

Since the cross-sectional area varies linearly from root to tip then (Ŗ= 1) and Eq (2.22) becomes;

$$A(z) = Ar - (Ar - At)(\frac{Z}{Lb}) \quad (2.28)$$

The centrifugal force as given by Eq. (2.20) and Eq (2.28) becomes:

$$F_{ef}(x) = \rho.\ \omega^2 \int_x^{Lb} [Ar - (Ar - At)(\frac{Z}{Lb})].(Rr + z).dz \quad (2.29)$$

Integrating Eq. (2.29) gives

$$F_{ef}(x) = \rho.\ \omega^2[Ar\ (Rr.z + \frac{Z^2}{2}) - \frac{(Ar-At)}{Lb}.(\frac{Rr.Z^2}{2} + \frac{Z^3}{3})]_x^{Lb} \quad (2.30)$$

When (x = 0) at the blade root, the centrifugal force is maximum and Eq. (2.29) becomes:

$$F_{ef}(0) = \rho.\ \omega^2[Ar\ (Rr.Lb + \frac{Lb^2}{2}) - (Ar - At)\ .\ (\frac{Rr.Lb}{2} + \frac{Lb^2}{3})] \quad (2.31)$$

And the maximum centrifugal stress is:

$$\sigma_{ef}(0) = \rho.\ \omega^2[(Rr.Lb + \frac{Lb^2}{2}) - (1 - \frac{At}{Ar}) . (\frac{Rr.Lb}{2} + \frac{Lb^2}{3})] \quad (2.32)$$

2.5Bending stresses: The moving blade experiences the bending force in addition to the centrifugal force. The bending force exerted by the working fluid on the moving blade is essentially a distributed load, which in the general case varies along the blade height. The impulse blade is subjected to bending from the tangential force exerted by the fluid [22]. Reaction blades have an additional bending force due to the large axial thrust because of the pressure drop which occurs in the blade passages. The blade without banding or lacing wire can be regarded as a cantilever beam of a variable cross-section area which is stressed by a distributed load (q(x)) as shown in figure 2.6 below. The components of aerodynamic force (q), is the axial force (qa) and the tangential force (qw) shown in the diagram, this force produces bending load on the blade.

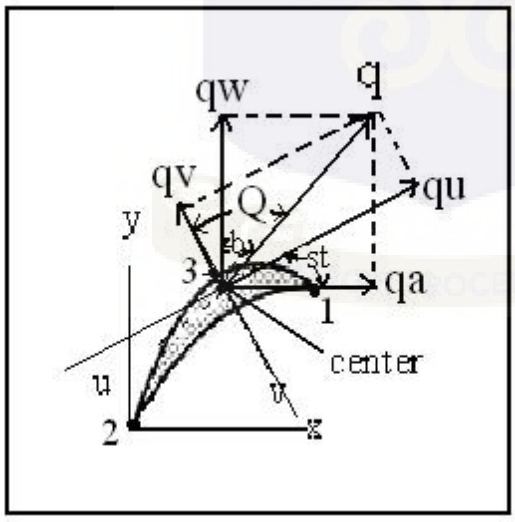

Fig. 2.6: A diagram showing the bending stress experienced by a blade, adapted from Atrens A, M. Muer, H. Meyer, G. Faber, and M.O. speidel

The moment of this force and the stress due to it are both maximum at the blade root. The bending stress diminishes with increase of the radius. If the blade is tapered, the bending

stress can be made to increase at greater radii. Consider the blade as cantilever beam fixed at the root section. The bending moment effect is on the level of the main axes of inertia (u, v) as shown above. The axial force [21].

$$qa = \rho f.cf_3\ (Vw_2 - Vw_3) \tag{2.33}$$

The tangential force [21]

$$qw = \rho_f.cf_3.\ (cf_2 - cf_3) + (P_2 - P_3).S \tag{2.34}$$

$$qw = (P_2 - P_3).S \tag{2.35}$$

The resultant force is

$$q = \sqrt{qw^2 + qa^2} \tag{2.36}$$

Where the component force on the main axes (u, v)

The force for the axis (u)

$$qu = q.\sin(Q) \tag{2.37}$$

The force for the axis (v)

$$qv = q.\cos(Q) \tag{2.38}$$

But Q is the angle between the force on the axis (v) and the result force shown above, then:

$$Q = b + st \tag{2.39}$$

$$b = \tan^{-1}\left(\frac{qa}{qw}\right) \tag{2.40}$$

$$st = \left[\tan^{-1}\left[\frac{-Ixy}{Ix-Iy}/2\right]/2\right] \tag{2.41}$$

The bending moment about axes (v, u) at any section of the blade height is;

$$Mv = \int_x^{Lb} qv(z).(z - x).dz \tag{2.42}$$

$$Mu = \int_x^{Lb} qu(z).(z - x).dz \tag{2.43}$$

The bending stress will be calculated for the following points in which the stress is maximum [22, 23] as shown above. For the entrance or leading edge of the blade, the stress is:

$$\sigma_{b1} = \frac{Mv*vv1}{Iu} + \frac{Mu*uu1}{Iv} \quad (2.44)$$

While for the exit or trailing edge;

$$\sigma_{b2} = \frac{Mv*vv2}{Iu} - \frac{Mu*uu2}{Iv} \quad (2.45)$$

And for a point located at the intersection of the v axis and the back of the blade which of course is subjected to compression stresses is:

$$\sigma_{b3} = -\frac{Mv*vv3}{Iu} \quad (2.46)$$

Where, the negative sign is for compression.

2.6 Total stresses: The total stress at a given point on a turbine blade may be found by adding the centrifugal stress at that point to the bending stress. The total stresses in leading edge point (1) as shown above are;

$$\sigma t1 = \sigma cf + \sigma b1 \quad (2.47)$$

The total stresses in trailing edge point (2) are;

$$\sigma t2 = \sigma cf + \sigma b2 \quad (2.48)$$

The total stresses in point (3) are;

$$\sigma t3 = \sigma cf + \sigma b3 \quad (2.49)$$

***2.7 Blade Terminology*:** It is necessary to define the parameters used in describing blade shape and configurations of blade. Blade profile are usually of airfoil shape for optimum performance, although cost is more important than the ultimate in efficiency, simple

geometrical shapes composed of circular areas and straight line are often used. The spacing or pitch of the blade is the distance between corresponding points of adjacent blade and is expressed either by the pitch chord ratio or alternatively the solidity. When the blades are evenly spaced around a rotor, the pitch is the circumference at any radius divided by the number of blades. The lift coefficient (CL) is found by using velocity diagram and the solidity [22].

$$CL = \frac{2.\triangleq Vw.S}{Vr} \tag{2.50}$$

$$CL = \frac{2.\triangleq Vw}{Cr.SO} \tag{2.51}$$

Solidity $(SO) = C/S$ (2.52)

Spacing $(C) = \frac{2.\pi.R}{Nb}$ (2.53)

The solidity factor (SO) depends on the chord and pitch of the blades. The pitch in turn depends on the number of blades used.

2.8 Blackbody radiation and the radiation laws

Kirchhoff (1895) examined the relationship between radiation absorbed and emitted by matter. He defined two separate terms in this relationship as absorptivity and emissivity. The absorptivity of a surface $\alpha(\lambda)$ is the fraction of incident radiation absorbed at a specific wavelength λ and the emissivity $\varepsilon(\lambda)$ as the ratio of the actual radiation emitted at a wavelength (λ) to a hypothetical amount of radiant flux **B (λ).** He considered that the thermal equilibrium of an object inside an enclosure at a uniform temperature, the absorptivity, $\alpha(\lambda)$ is always equal to the emissivity, $\varepsilon(\lambda)$. In the case of an object where the emissivity $\varepsilon(\lambda)$=1 at all wavelengths, the spectrum of the emitted radiation is known as a black body spectrum. Kirchhoff's radiation law is represented mathematically as;

$$\alpha(\lambda) = \varepsilon(\lambda) \tag{2.54}$$

Kirchhoff law (2.2) indicates that, at the same wavelength, good emitters are equally good absorbers.

The basic law of radiant emission of energy is the Planck's law (1900) which is given as

$$E_\lambda * = c_1/[\lambda^5(\exp(\frac{c_1}{\lambda T}) - 1) \tag{2.55}$$

Where $E_\lambda *$= amount of energy $Wm^{-2}\mu m^{-1}$ emitted at wavelength $\lambda(\mu m)$ at temperature T (K)

$c_1 and\ c_2$=3.0 $\times 10^8 ms^{-1}$and $\lambda(\mu m) = 1.44 \times 10^4 \mu m.$

This law is clearly stated as "A fundamental law of quantum theory where the energy associated with electromagnetic radiation is emitted or absorbed in discrete amounts which are proportional to the frequency of radiation.

Wien's (1896) deduced that the maximum energy per unit wavelength should be emitted at a wavelength λ_m given by;

$$\lambda_m = \frac{2897}{T}\ \mu m \tag{2.56}$$

Where T= temperature and $\lambda =$ wavelength.

This law takes into consideration measurements using a combination of a spectrometer and a sensitive thermopile thereby establishing that the spectral distribution of radiation from a full radiator is a curve in which the chosen temperatures of 6000K and 300K correspond approximately to the black body temperatures of the sun and the earth's surface (Henderson and Robinson, 1994).

Stefan-Boltzmann also formulated a law that related the Energy flux density being proportional to the fourth power of its absolute temperature. Because the energy flux density is proportional to the fourth power of its temperature, emission of radiation from earthly bodies changes considerably, even in the limited temperature range characteristic of a single day or a short season. The law can be mathematically stated as;

$$E = \sigma T^4 \tag{2.57}$$

Where E= energy flux density, σ = Boltzmann's constant which is $5.67 \times 10^{-8} Wm^{-2}K^{-1}$ and T is the temperature measured in kelvin.

From the stated laws and principles, it is clear that the flux density and wavelength of maximum emission are functions of the temperature of the radiating body.

2.9 The cosine law of emission and absorption

The temperature which determines the total flux of energy emitted by a surface can be estimated by measuring the radiance of the surface with an appropriate equipment.

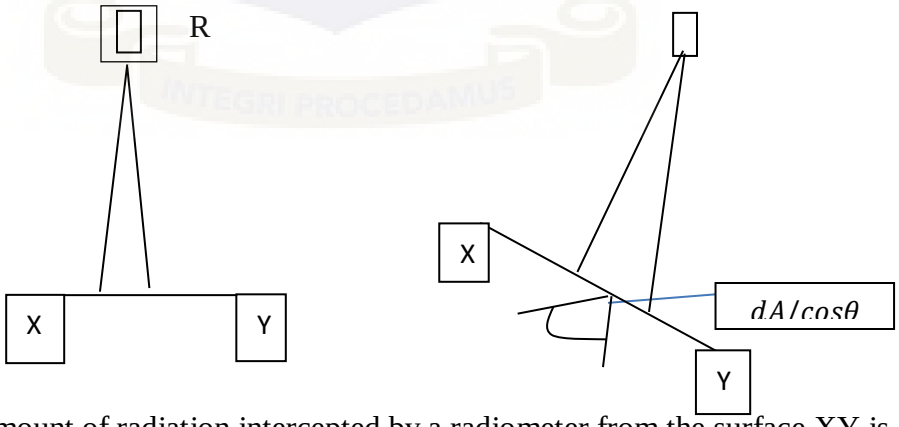

Fig. 2.7: The amount of radiation intercepted by a radiometer from the surface XY is independent of the angle of emission, but the flux emitted per unit area is proportional to cosθ. (Adapted from Monteith, 1973)

As the source of a full radiator will appear to have the same temperature whatever angle it is viewed from, the intensity of radiation emitted from a point source on the surface and the radiation of an element of surface must both be independent of θ. On the other hand, the flux per unit solid angle divided by the true area of the surface must be proportional to $cos\theta$ as shown in the figure above. A radiometer R mounted vertically above an extended horizontal surface XY sees an area,dA. When the surface is tilted through an angle, θ, the radiometer now sees a larger surface $dA/cos\theta$, but provided the temperature of the surface stays the same, its radiance will be constant and the flux recorded by the radiometer will also be constant. It therefore follows that the flux emitted per unit area (the emitance of the surface) at an angle θ must be proportional to $cos\theta$ so that the product of emitance and the area emitting to the instrument stays the same for all values of θ as illustrated in figure 2.7.

CHAPTER THREE

3.0 METHODOLOGY

In this chapter we present a complete set-up of our low pressure steam turbine and how its capability has been demonstrated. As already stated, this turbine is comparable to the ones previously developed in other laboratories [30]. First, the experiment set up and alignment procedure are described. Then, specific construction techniques that were implemented to yield improvements are discussed. The turbine is the work engine and must be field producible. A boundary layer turbine was a promising design because it can be efficient at low operating pressures and is the very straightforward to construct. The design and construction of Tesla turbines employed 2D (sheet) metals and plastics and used the least number as possible of prefabricated special parts such as springs, bearings, and fasteners. Various industries have built boundary layer turbines for both shaft work and electrical generation applications. Most turbines are large with 6" to 24" diameter disks and are generally hydro or wet steam powered.

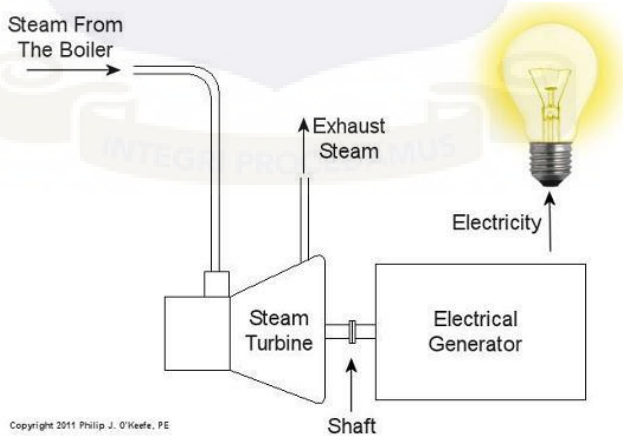

Fig. 3.1 A diagram showing the three phases of the project

Historical rotor efficiency has been reported to be 97%. Modern analysis of Tesla's design shows

the rotor to be more than 95% efficient at fluid to rotary motion transfer. The entire engine was 36% efficient overall with most of the losses found to be heat lost at the inlet and outlet [31]. Improved modern designs include improved seals and nozzles which can increase the overall efficiency.

3. 1 Design and Construction

The entire project is in three phases as shown in figure 3.1. Thus, the construction of the boiler, the solar concentrator , and then the turbine. The sun's energy converted water to steam, in our case a pressurized tank was used to generate the steam and ran the turbine off the steam. The design and construction of this low pressure steam turbines employed 2D (sheet) aluminum metal of thickness 0.06mm, two cylindrical metal containers as the casing, a copper pipe rod as the rotating shaft, two metal bearings, a rotor and a stator of 16 and 8 blades respectively, fibre glass and a wooden base.

3.2 Turbine cylinders

For the design of this turbine, two cylindrical aluminum containers as shown in figure 3.2 were used. This particular material was chosen due to low temperature gradients within its rigid components, and its ability to withstand high thermal stresses.

Fig. 3.2 A picture of two cylindrical containers

Also during heating and cooling the temperature gradients become particularly adverse as larger parts take longer to change their temperature than smaller parts, so all these were taken into consideration before the cylinder was chosen. Again in order to assemble the turbine and to disassemble it for maintenance, the two cylinders were joined horizontally as indicated in figure 3.3 and sealed to prevent the loss of the steam and the pressure and to make way for maintenance as well.

Fig. 3.3: Two containers joined horizontally using strips of aluminum sheets

Since the shaft of the rotor passes through the end of the casing, a small hole was created at the centers of the casing and a sealant was applied to prevent steam leakage.

3.3 Rotor and Stator

Six blades comprising of three rotating blades (the rotors) and three other stationary ones (the stators) were designed and constructed, with each having a 9” diameter, 0.06” thick aluminum sheet as shown in figure 3.4 below. A number of considerations were made before the construction, since it is the critical element of the turbine. [19]

Fig. 3.4: A Picture rotor blades constructed

Due to its unique function, the blades were designed in such a way that it has an airfoil shape with an angle of 90^0 getting to the tip of the blades. So that when fluid passes through stator blades velocity of fluid increase due to its special shape thus one part of enthalpy energy will get converted into kinetic energy. Thus enthalpy of steam reduces and kinetic energy of stream increase.

Fig. 3.5: A picture of rotors, stators and shaft

As indicated in figure 3.5 above, the shaft of the rotors was carried on the bearings and are linked together and to the electrical generator. The bearings were properly aligned to accommodate the natural gravitational bending of the shaft. Allowance were also made for differential expansion between the rotors and the casing during thermal transients. And since both must be free to expand without upsetting the alignment, while allowing the rotors to expand more quickly and to greater degree than the casing, lubrication was ensured, especially for the bearings. To ensure effective and uniform rotation of the turbine blades, two small bearings were fixed at the extreme ends of the shaft to enhance the rotation of the rotors as shown in figure 3.6.

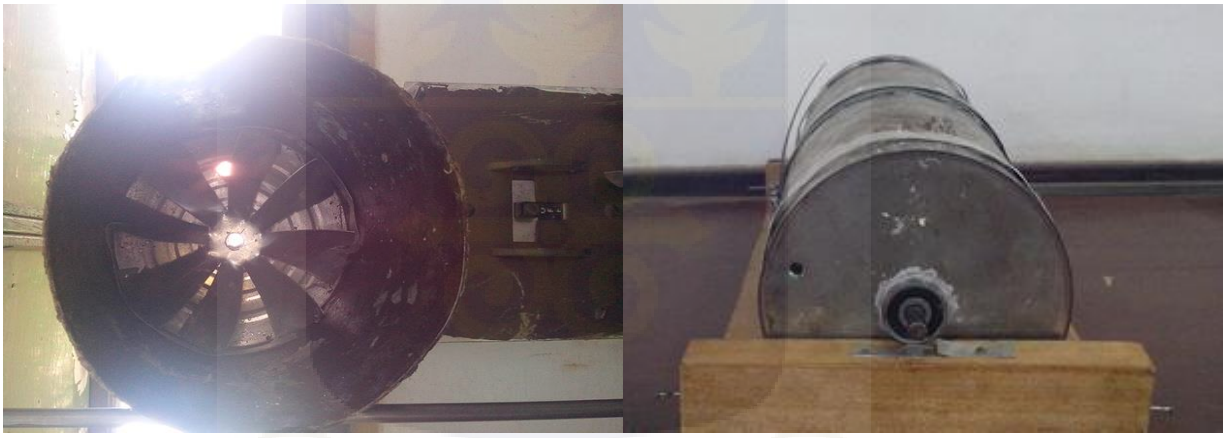

Fig. 3.6: A picture showing a fixed stator in a casing and the attachment of a steel bearing.

The bearings posed the greatest source of frictional losses for the system and will require further research and experimentation to minimize their loss effects on the system.

3.4 Insulation

And to ensure effective use of the steam, the entire system was insulated with fibre glass as shown in figure 3.7, so that heat loss to other parts of the turbine would be minimized.

Fig. 3.7: A picture of a hollow and an insulated system

3.5 Testing and Operation

Steam turbines belong to power generating turbo machines which uses the steam as a working fluid. In steam turbines, high pressure steam from the boiler is expanded in nozzle, in which the enthalpy of steam being converted into kinetic energy. Thus, the steam at high velocity at the exit of nozzle impinges over the moving blades which cause to change the flow direction of steam and thus cause a tangential force on the rotor blades. When fluid passes through rotor blades it loses some amount of energy to the rotor blades. Due to this both kinetic and enthalpy energy of fluid come down for a typical rotor. As kinetic energy comes down velocity of flow decreases. If we directly pass this stream to next stage of rotor blades it will not transfer much energy because of low velocity of flow stream. So before passing the steam to next rotor stage we have to increase the velocity first. This is achieved with the use of a set of stationary nozzle blades, stator.

In this project, due to the unavailability of the solar concentrator, a low pressure steam was generated using boiling water in a tank. The pressure was then trapped to about 40psi, which was then fed into the turbine. This amount of pressure was able to cause rotation of the rotor. The setup in figure 3.8, shows how the low pressure steam was generated.

Fig. 3.8: A picture showing the experimental setup of the project

CHAPTER FOUR

RESULT AND DISCUSSION

4.0 Introduction

In this chapter, the results obtained from the observations made when various amount of steam were fed into the turbine over the study period are presented and thoroughly analyzed to ascertain possible relationships between them. The under listed formulas were used for the calculation of the stated parameters;

The mass flow rate of steam, $ms = \frac{Q2}{h2 - hf3}$ (kg/h)

The power output of turbine, $P = \frac{ms\ (h1 - h2)}{3600}$ (kw)

The thermal efficiency of the turbine, ηs $= \frac{h1 - h2}{h1 - hf2}$

The work done on the turbine, $WT = h_1 - h_2$ (kJ/kg)

Where Q_2 is the heat lost by steam

$h_1$and h_2 are the values of entrance enthalpy and exit enthalpy from the turbine respectively..

Again the specific steam consumption which is the steam consumed by turbine cylinders per unit output of power was also calculated.

Specific Steam Consumption, SSC = $\frac{3600}{Wnet}$ (kg/kWh)

4.1 Calculation of solar radiation

The solar radiation is an instantaneous power density in units of kW/m^2. The solar radiance varies throughout the day from 0 kW/m^2 at night to a maximum of about 1 kW/m^2. According to the Stefan-Boltzmann equation that is $j = \sigma T^4$. The irradiance j is

proportional to the fourth power of the absolute temperature T. The proportionality constant σ which is equal to 5.67 x 10^{-8} W/ (m^2K^4), i.e. 56.7 nanowatt per square meter and per quartic Kelvin.

Considering the average temperature of 15 °C i.e. 273+15 = 288 Kelvin.

That is 288^4 x 5.67 x 10^{-8} W/ (m^2K^4) = 390.08Watt/m^2**.** Because of the (mostly natural) greenhouse effect, albedo, and related effects, the relevant average solar irradiance is about 342 Watt/m^2. Therefore using a solar concentrator of 10 square meters would generate enough power for the operation of the low steam turbine constructed.

Measured operating parameters which include specific steam consumption, turbine inlet and outlet temperatures, turbine input and output pressure, heat flow, thermal efficiency and boiler's output pressure were processed in Matlab environment.

4.2 Discussion

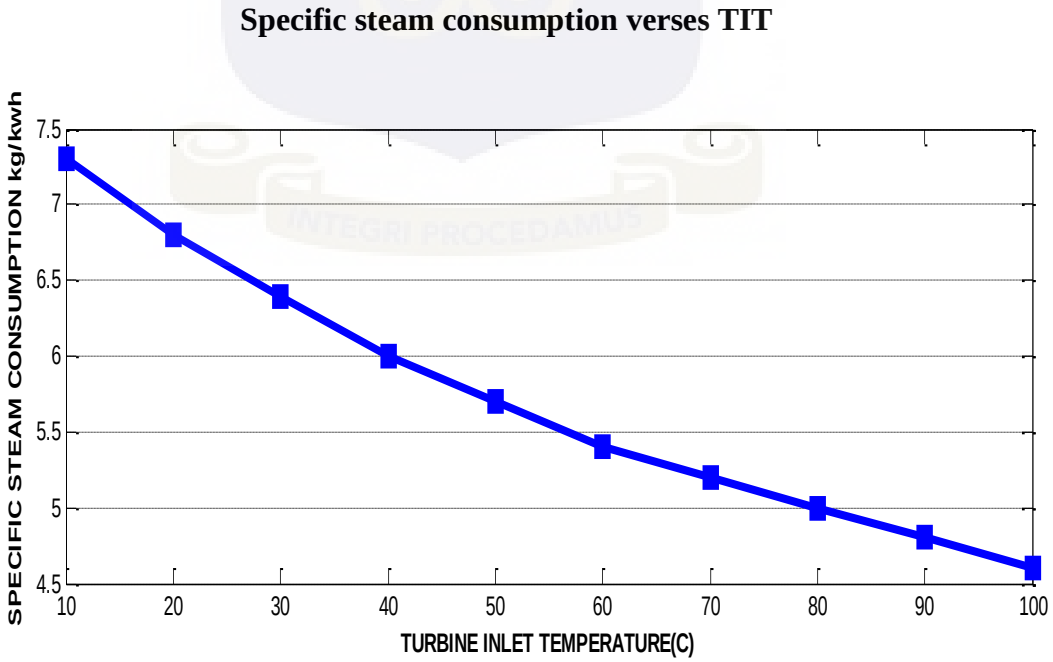

Fig. 4.1: A graph showing variation of specific steam consumption with turbine

inlet temperature.

The fig 4.1 shows the variation of specific steam consumption with turbine inlet temperature. Raising the inlet steam temperature also reduces the wetness of the steam in the later stages of the turbine and decreases specific steam consumption. At lower temperature, enthalpy will be low, work done by the turbine will be low, turbine efficiency will be low, hence steam consumption for the required output will be higher. In other words, at higher steam inlet temperature, heat extraction by the turbine will be higher and hence for the required output, steam consumption will reduce.

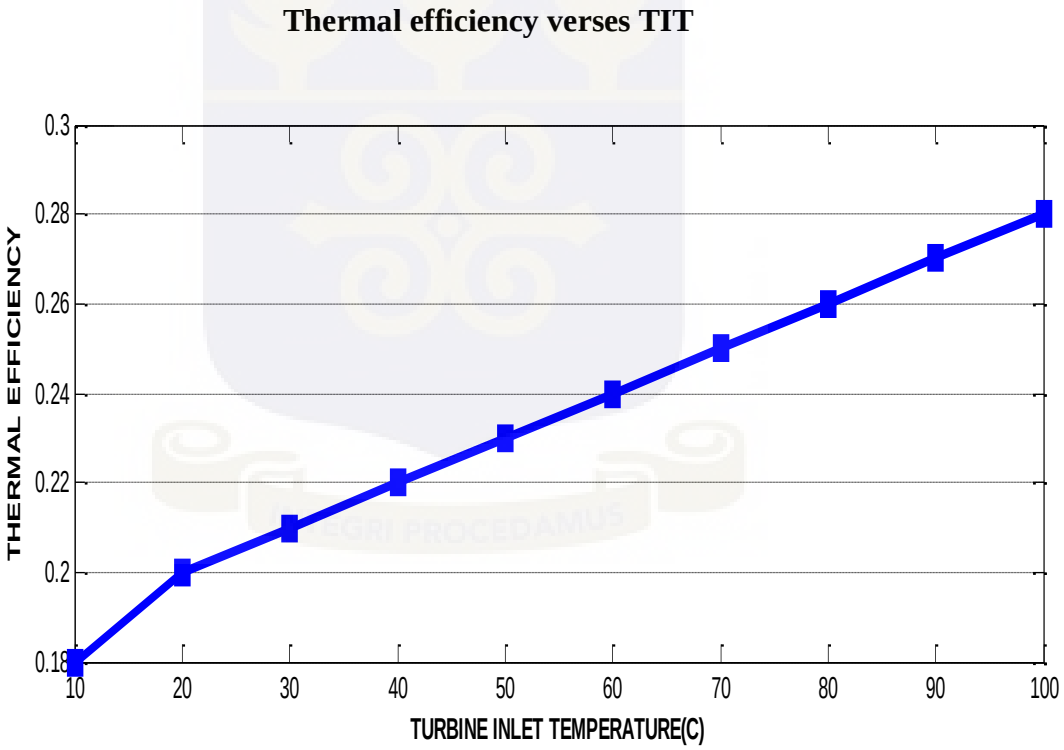

Fig. 4.2: A graph showing variation of the thermal efficiency with turbine inlet temperature.

Again fig 4.2 shows the variation of the thermal efficiency with turbine inlet temperature. The increase in turbine inlet temperature means an increase in superheat at constant inlet

steam pressure and condenser pressure gives a steady improvement in the thermal efficiency of the cycle. Raising the inlet steam temperature also reduces the wetness of the steam in the later stages of the turbine and improves the turbine internal efficiency. In steam cycle, the thermal efficiency increases gradually with increase in turbine inlet steam temperature which thereby increases the quality of steam at the turbine exhaust.

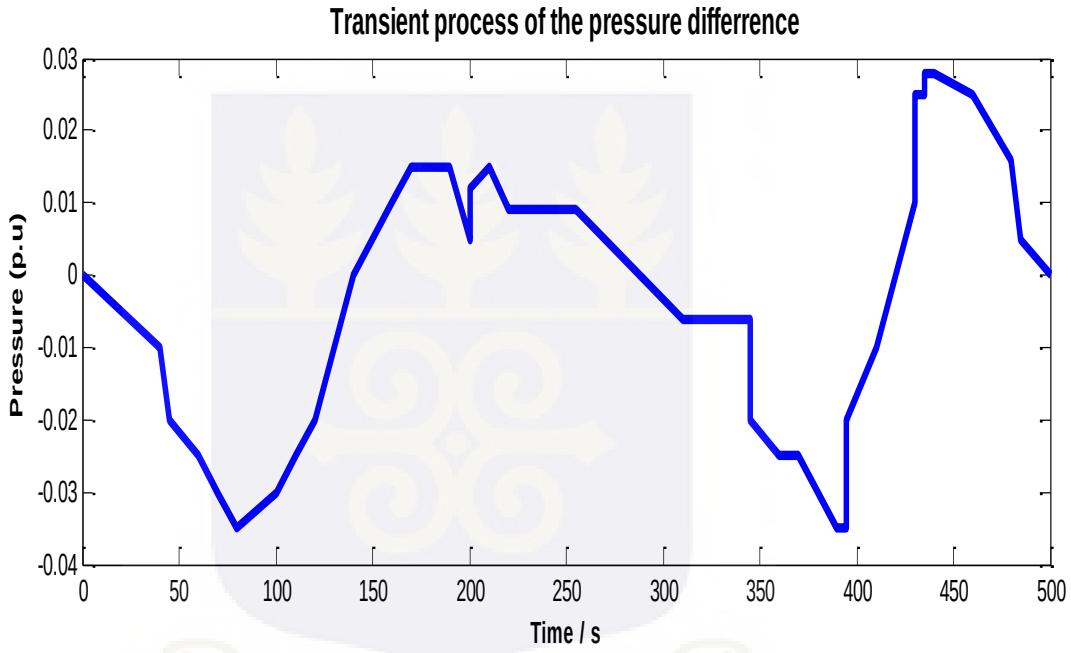

Fig. 4.3: A graph showing the transient processes of pressure difference (input)

Pressure is maximum at the being , that is inlet to stator blade and the pressure drops as the steam passes through the stator blades and the rotor blade, the pressure drops, as the working medium passes through the stator and rotor blades as shown in figure 4.3, this condition satisfies Impulse-reaction turbine.

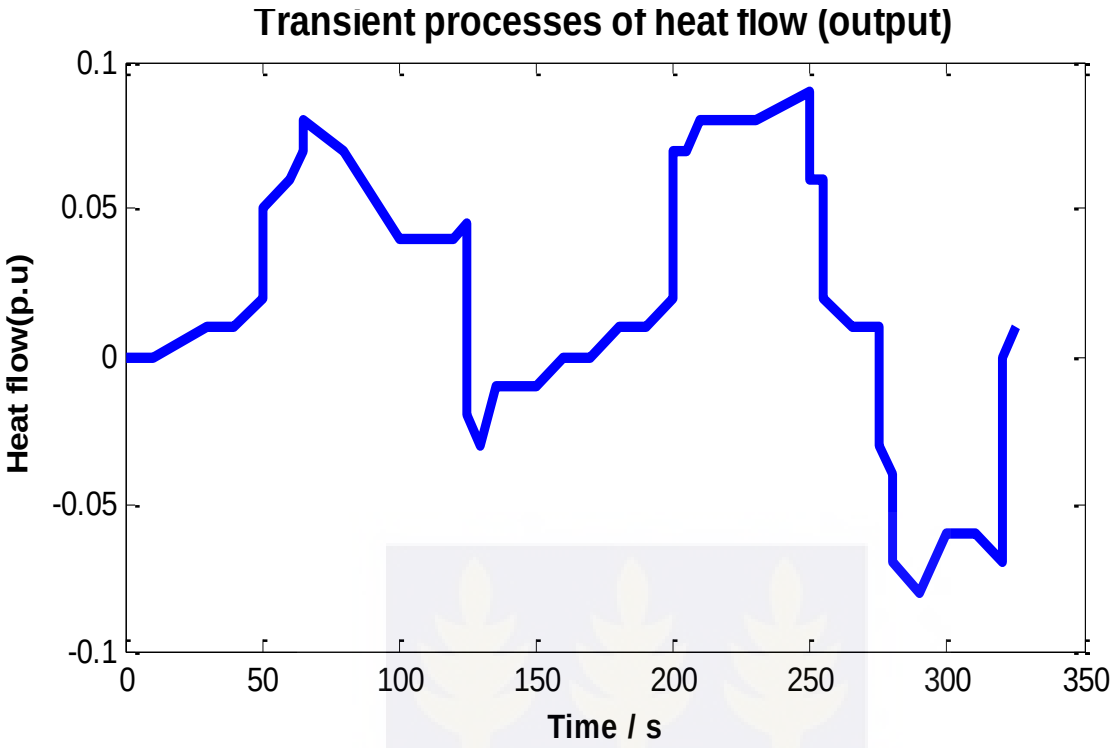

Fig. 4.4: A graph of transient processes of heat flow (output).

The heat flow at the initial state was high as it can be seen in figure 4.4 above and this is as a result of the inlet temperature, but as it flows through the various stage of the turbine, some of the energy is being absorbed by the blades which reduces the heat flow at the output which affect the performance of the turbine.

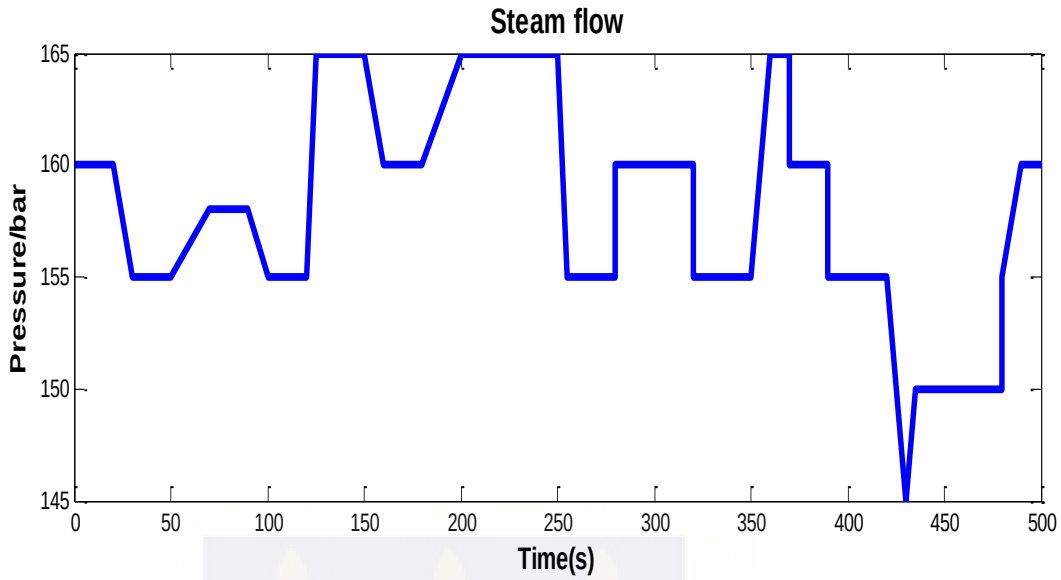

Fig. 4.5: A graph showing variation of measured steam flow in the turbine.

The steam flow rate in the turbine was also was also measured and the figure 4.5 depicts the outcome. The temperature of the heat was varying due to the arrangement of the rotors and the stators which absorb the greater portion of the energy.

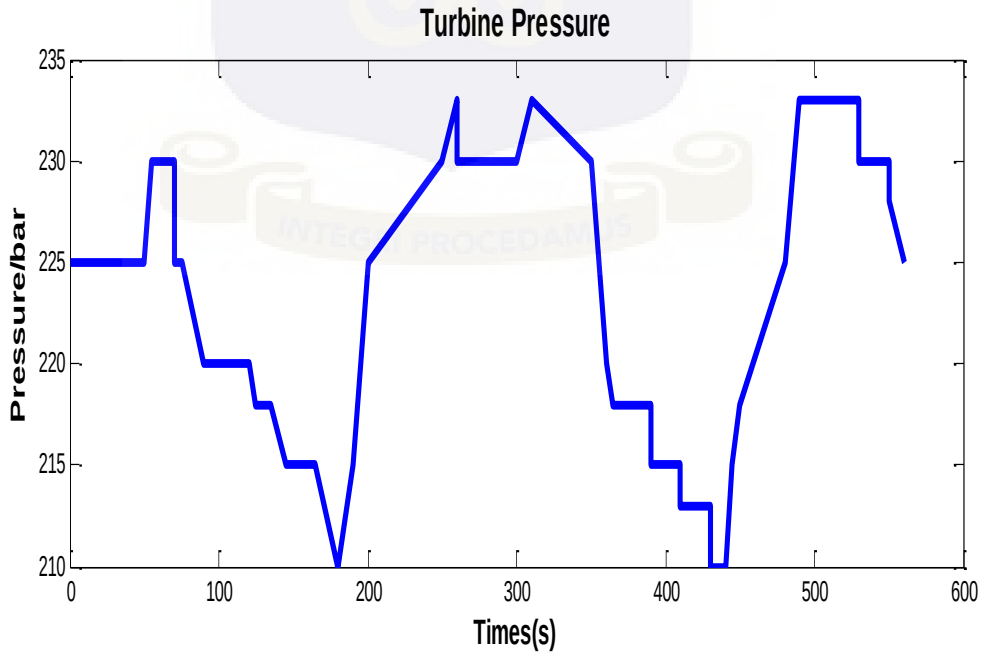

Fig. 4.6: A graph showing variation of measured turbine pressure

A pressure drop occurs across both the stator and the rotor, with steam accelerating through the stator and decelerating through the rotor as depicted in figure 4.6, with no net change in steam velocity across the stage velocity across the stage but with decrease in both pressure and temperature, reflecting the work performed in the driving of the rotor.

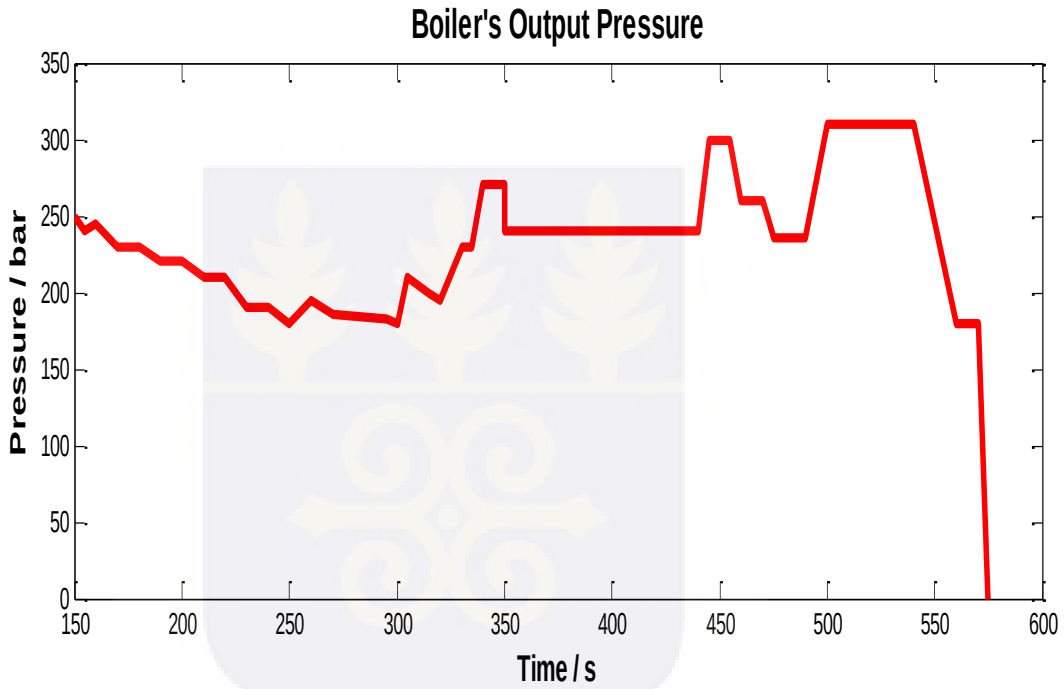

Fig. 4.7: A graph showing variation of measured boiler's output pressure.

Pressure is maximum at the early stage from the figure 4.7 but decreases as it passes through the system which decrease the overall thermal efficiency of the steam generating system because the higer steam temperature requires a higher steam exhaust temperature.

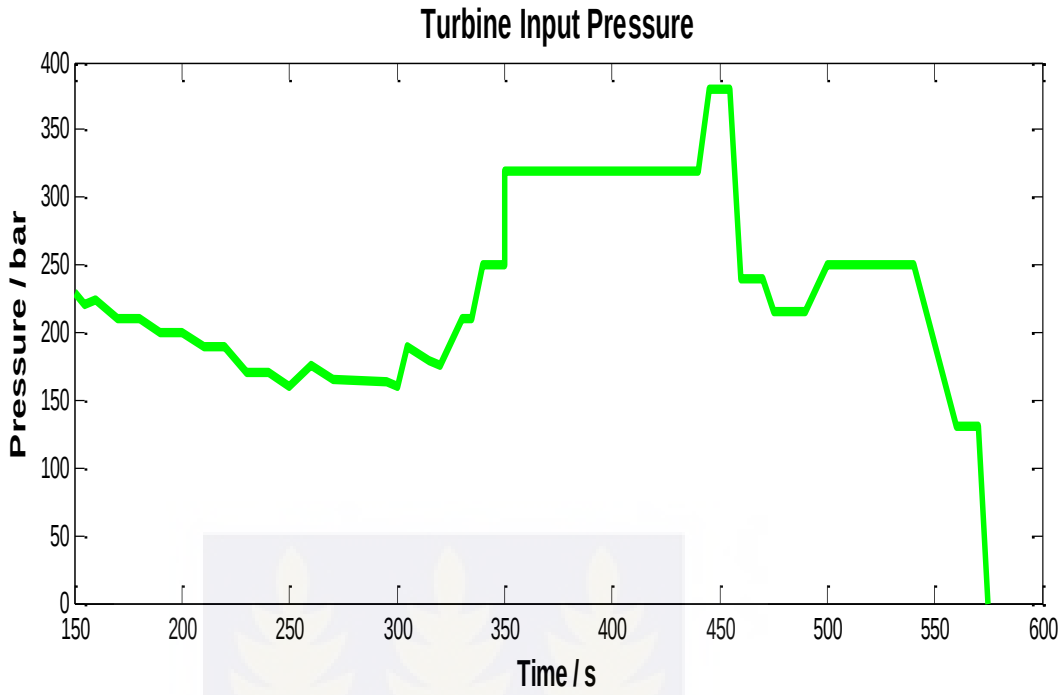

Fig. 4.9: A graph showing variation of measured turbine input pressure

Pressure drop completely, when the fluid passes over the moving blades, pressure drop does not take place again. Hence pressure remains constant when the fluid passes over the moving blades. As the steam flows through the nozzle its pressure falls from inlet pressure to the exit pressure as it can be seen in figure 4.9.

CHAPTER 5

5.0 CONCLUSION

The low pressure steam turbine was constructed and it can be stated that the consideration in determining the performance of a steam turbine was evaluated. Parametric study showed that turbine inlet temperature played a very vital role on the performance of a steam turbine in terms of power output of the turbine, thermal efficiency and specific steam consumption. From the data obtained during the experimental operation of the turbine, temperature is maximum at the beginning, that is at inlet to the first stator blade and is around 88^{o}C and the temperature at the exit of the turbine is 59.5^{0}C. The maximum steam velocity at the inlet of the moving blade is 256 m/s and the velocity of steam at the exit of stage is 42 m/s. From the analysis we can conclude that the power output and the thermal efficiency are highest when turbine inlet temperature is increased and the specific steam consumption is least with the increase in turbine inlet temperature. The satisfactory performance at low steam pressure demonstrates that this turbine may be applied in solar-thermal based power generation application where steam pressures are usually low.

5.1 RECOMMENDATIONS

We recommend that in the designing and construction of such a system;

1. Proper insulation materials like the fibre glass must be used to minimize the amount of losses in energy of steam which occur inside and outside of the turbine.

2. Material selected for blades must either be plastics or coated metals to avoid corrosion.

3. In selecting the area for the operation of solar powered turbine,one year measurement of global solar radiation in the study area should be carried out. This will help to determine the seasonal variation of solar radiation at the particular location.

4. More research activities should be encouraged in the field of fabrication of solar collectors to ensure maximum collection of solar radiations.

REFERENCES

1. Energy Information Administration, Renewable Energy Consumption and Electricity Preliminary Statistics 2008, online:http://tonto.eia.doe.gov/energyfacts/images/charts/role_of_renewables_in_us_energy_large.png

2. G. Knies, U. Möller, M. Straub, 2007, *Clean Power from Deserts: The DESERTEC Concept for Energy, Water and Climate Security*, Trans- Mediterranean Renewable Energy Cooperation, Hamburg

3. European Commission, 2010, *The European Strategic Energy Technology Plan (SET-Plan)*, European Commission Research and Innovation, ec.europa.eu/research/energy (accessed 4th December 2012)

4. International Energy Agency, 2010, *Technology Roadmap: Concentrating Solar Power*, IEA Publications, OECD/IEA, Paris

5. International Energy Agency, 2010, *Technology Roadmap: Solar Photovoltaic Energy*, IEA Publications, OECD/IEA, Paris

6. International Energy Agency, 2011, *Renewable Energy Technologies: Solar Energy Perspectives*, IEA Publications, OECD/IEA, Paris.

7. International Energy Agency, 2011, *Harnessing Variable Renewables: A Guide to the Balancing Challenge*, IEA Publications, OECD/IEA, Paris

8. Amy Sun.," Field Fabrication of Solar-Thermal Powered Steam Turbines for Generation of Mechanical Power", Dual B.S. Computer and Electrical Engineering, Purdue University in West Lafayette, Indiana (1996).

9. Ruedisili, Lon C. Perspectives on Energy. Oxford University Press, 1978.

10. Harding Energy Inc. Battery Technology Handbook. 2004.

11. Dutton, E.G and J.J Michalsky, T. Stoffel, B.W. Forgan, J. Hickey, T. L. Alberta, I. Reda (2001): *Measurement of broadband diffuse solar irradiance using current commercial instrumentation with a correlation for thermal offset error*, Journal of Atmospheric and Oceanic Technology, 18(3), pp. 297-413.

12. Szász, Gábor, Tőkei, László (1997): Meteorológiamezőgazdáknak, kertészeknek, erdészeknek. ["*Meteorology for farmers, gardeners and foresters*"], MezőgazdaKiadó, Budapest. Vol. 3. Pp. 164-166.

13. Salam Abdel, A.S., Higazy, N.A., VezirogluNejat, T. (1978): *Solar data application to Egypt, Proceedings of the International Symposium Workshop on Solar energy*, Vol.1. pp. 20-40.

14. Gueymard, C.A. (2004): *The sun's total and spectral irradiance for solar energy applications and solar radiation models*, solar energy, Vol. 74(6). pp. 423-453.

15. Fröhlich, C. and Judith, L. (1998): *The sun's total irradiance: cycles, trends and related climate change uncertainties since 1976*, Geophysical Research Letters, Vol. 25(23), pp. 4377-4380.

16. Dutton, E.G and J.J Michalsky, T. Stoffel, B.W. Forgan, J. Hickey, T. L. Alberta, I. Reda (2001): *Measurement of broadband diffuse solar irradiance using current commercial instrumentation with a correlation for thermal offset error*, Journal of Atmospheric and Oceanic Technology, 18(3), pp. 297-413.

17. Stoffel, T. and Wilcox, S. (2004): Solar radiation measurements: A workshop for the national association of state universities and land grant colleges, NREL.

18. Khadir MT, Klai S (2010). A steam turbine diagnostic maintenance system based on an evolutive domain ontology. International Conference on Machine and Web Intelligence (ICMWI). pp. 360-367.

19. Yufeng M, Yibing L (2011). AnHongwen; Statistical analysis of steam turbine faults. International Conference on Mechatronics and Automation (ICMA). pp. 2413-2417.

20. Qing H, Dongmei D, Hong L (2006). Research on Web System of Intelligent Diagnosis for Steam Turbine. Chinese Control Conference (CCC2006). pp. 1271-1275.

21. Klure-Jensen J, Hanisch R (1991). Integration of steam turbine controls into power plant systems. IEEE Trans. Energy Convers. 6(1):177-185.

22. Bize LN, Hurley JD (1999). Frequency control considerations for modern steam and combustion turbines. IEEE Power Eng. Soc. Winter Meet. 1:548-553.

23. Chowdhury AA, Koval DO (2006). Causal Analysis of Distribution System Reliability Performance. IEEE Ind. Commer. Power Syst. Tech. Conf. pp. 1-7.

24. Jianmei W, Kai C, Xinqiang M (2008). Optimization Management of Overhaul and Maintenance Process for Steam Turbine. ICIII'08. 3:244- 247.

25.[http://www.roymech.co.uk/Related/Thermos/Thermos_Steam_Turbine.html]

26. Rice, W. *Tesla Turbomachinery*. Proceedings of the SASA IV International Tesla Symposium; Belgrade, Yugoslavia, Sept 2225, 1991

27. Biomass Boundary Layer Turbine Power System, http://eisg.sdsu.edu/Far/0006 FAR Appendix A.pdf.

28. http://www.iaus.com/navajomountain.htm.

29. The outlook on renewable Energy in (ACORE), January 2007.

30. D. Kammen, \What solar power needs now," *Renewable Energy Access*, August 2007.

31. Miller, Gerald E. A Multiple Disk Centrifugal Pump as a Blood Flow Device. IEEE Transactions on Biomedical Engineering. Vol 7, No 2. February 1990.

32. Kostyok, A., and Frolov, V., "Steam and Gas Turbine, English Translation, Mir Publisher, Moscow, 1988.

33. Edwin, F. Church, "Steam Turbine", McGraw-Hill Book Company Inc., sept 1981, pp. (4 – 50) – (4 – 68).

34. Atrens A, M. Muer, H. Meyer, G. Faber, and M.O. speidel, "BBC Experience with Low – Pressure Steam turbine", workshop Proceedings, Palo alto, California, Corrosion Failure of steam Turbine blade materials, Sept. 1981, pp. (4 – 50) – (4 – 68)

35. Kadambi, J.R., Quinn, R.D., and Adams, M.L, "Turbomachine Blade static stress Measurements utilizing Nonintrusive techniques", Journal of Turbomachinery, Vol. 111, No.4, Oct. 1989, pp.468 – 474.

36. John F. Lee, "Theory and Design of steam and Gas Turbines", McGraw- Hill Book Company Inc.,1954.

37. Mukherjee, D. K., "Stresses in Turbine Blade due to temperature and load variation", ASME Paper No. 48-GT, 1988, 158pp.

38. Bakhtar, F., So, K.S., " A Study of Nucleating Flow of Steam in a Cascade of Supersonic Blading by the Time-Marching Method", International Journal oh Heat and Fluid Flow, Vol. 12, pp: 52-64., 1991

39. Deckers, M., Simon, V., Scheuerer, G., "The Application of CFD to Advanced Steam Turbine Design", International Journal of Computer Applications Technology, 1997.

40. Zamri, M.Y., " An Improved Treatment of Two-Dimensional Two-Phase Flows of Steam by a Runge-Kutta Method", Ph.D. Thesis, Department of Manufacturing and Mechanical Engineering, The University of Birmingham, U.K., 1997

41. www.freepatentonline.com

42. G.P. Wozney, M. Akiba, G.L. Touchton, R.I. Jaffee, S.J. Woodcock, "Turbine Research and Development for Improved Coal-Fired Power Plants", American Power Conference, April 14-16, 1986.

42. K.M. Retzlaff and K. Aizawa, "Turbine Designs", First International Conference on Improved Coal-Fired Power Plants, November 19-21, 1986.

43. Stoffel, T. and Wilcox, S. (2004): *Solar radiation measurements: A workshop for the national association of state universities and land grant colleges, NREL*.

APPENDIX

Turbine inlet temperature	Turbine outlet tempereature	Specific stem consumption	Thermal efficiency
20.4	0.2	7.2	0.18
28.3	0.6	6.7	0.2
31.6	0.9	6.2	0.21
48.6	11.6	5.5	0.22
57.5	20.1	5.2	0.23
68.4	28.0	4.7	0.24
73.4	33.2	4.6	0.25
78.2	53.7	4.5	0.26
80.6	58.4	4.4	0.27
88.0	59.5	4.4	0.28

A1 Table of Turbine temperature against specific stem consumption and thermal efficiency

Heat flow (p.u)	Time/s	Heat flow (p.u)	Time/s
0	0	0	170
0	0	0.01	180
0.01	30	0.02	190
0.01	40	0.07	200
0.02	50	0.07	200
0.03	50	0.08	205
0.04	50	0.08	210
0.05	50	0.09	230
0.06	60	0.06	250
0.07	65	0.06	250
0.08	65	0.02	255
0.07	80	0.01	255
0.04	100	0.01	265
0.04	120	-0.03	275
0.045	125	-0.04	275
-0.02	125	-0.07	280
-0.03	130	-0.08	280
-0.01	135	-0.06	290
-0.01	150	-0.06	300
0	160	-0.07	310

		0	320

A3. Table of Pressure against time

Time/s	Pressure	Time/s	Pressure
150	250	315	200
155	240	320	195
160	245	330	230
170	230	335	230
180	230	340	270
190	220	350	270
200	220	440	240
210	210	445	240
220	210	455	300
230	190	470	300
240	190	475	260
250	180	490	260
260	195	500	235
270	185	540	235
295	183	560	310
300	180	570	180

Pressure/bar	Time/s	Pressure/bar	Time/s
225	0	225	355
225	50	220	360
230	49	218	365
230	50	218	390
225	55	215	390
225	70	215	410
220	75	213	410
220	90	213	430
218	120	210	430
218	125	210	440
215	135	215	445
215	145	218	450
210	165	225	480
215	180	233	490
220	190	233	530
225	195	230	530
230	200	230	550
233	250	228	550
230	260	225	560
230	260		
233	300		
230	350		

305	210	575	0

A4 Pressure against time (boiler output)

Time	Pressure	Time	Pressure
150	230	315	210
155	220	320	210
160	225	330	250
170	210	335	250
180	210	340	320
190	200	350	320
200	200	440	380
210	190	445	380
220	190	455	240
230	160	470	240
240	175	475	215
250	165	490	215
260	163	500	250
270	160	540	250
295	190	560	130
300	180	570	130
305	175	575	0

A5 Pressure against time (turbine input pressure)

Time/s	Pressure/bar	Time/s	Pressure/bar
150	200	315	150
155	190	320	145
160	195	330	180
170	180	335	180
180	180	340	220
190	170	350	220
200	170	440	190
210	160	445	190
220	160	455	250
230	140	470	210
240	140	475	210
250	130	490	185
260	145	500	185
270	135	540	260
295	133	560	260

300	130	570	130
305	160	575	0

A6 Pressure against time (turbine power)

Steam Velocity (Inlet)	Steam Velocity (Outlet)
25.4	12.8
57.8	22.6
81.3	26.5
100.5	28.4
141.5	31.3
173.4	36.4
202.7	38.6
232.4	40.0
256.0	42.1

A7 Steam velocity (Inlet) against steam velocity (outlet)

ABBREVIATIONS AND ACRONYM

(TWhe)	Terawatt Hour of electricity
GW	Gigawatt
NiMH	Nickelmetalhydride
AM0	Air mass zero
BTU	British thermal units
PV	Photovoltaic
HP	High pressure turbine
IP	Intermediate pressure
MW	megawatt
DHIHP	isotropy difference enthalpy
DHRHP	real difference enthalpy
H_{vap}	enthalpy of steam overheated admission HP turbine
H_{erh}	enthalpy of steam to overheat HP exit
H_{ith}	final enthalpy
CL	lift coefficient
SO	solidity factor
C	Spacing
E	energy flux density
ms	mass flow rate of steam
P	power output of turbine
ηs	thermal efficiency of the turbine
WT	work done on the turbine
Q	Heat lost by system
SSC	Specific Steam Consumption